AEC RESEARCH AND
DEVELOPMENT REPORT

HW-69401

METALLOGRAPHIC STUDY OF THE ANNEALING BEHAVIOR OF ALUMINUM-SILICON EUTECTIC ALLOY

R. H. TODD

JUNE, 1961

HANFORD LABORATORIES

HANFORD ATOMIC PRODUCTS OPERATION
RICHLAND, WASHINGTON

GENERAL ELECTRIC

LEGAL NOTICE

AEC-GE RICHLAND, WASH.

HW-69401

UC-25, Metals, Ceramics
and Materials
(TID-4500, 16th Ed.)

METALLOGRAPHIC STUDY OF THE ANNEALING BEHAVIOR OF ALUMINUM-SILICON EUTECTIC ALLOY

By

R. H. Todd

Materials Development
Reactor and Fuels Research and Development
Hanford Laboratories

June, 1961

HANFORD ATOMIC PRODUCTS OPERATION
RICHLAND, WASHINGTON

Work performed under Contract No. AT(45-1)-1350 between the Atomic Energy Commission and General Electric Company

Printed by/for the U. S. Atomic Energy Commission

TABLE OF CONTENTS

METALLOGRAPHIC STUDY OF THE ANNEALING BEHAVIOR OF ALUMINUM-SILICON EUTECTIC ALLOY

INTRODUCTION

The silicon phase of an aluminum-silicon (Al-Si) eutectic alloy has shown a definite tendency to spheroidize after prolonged exposure at moderate temperatures.[1] Silicon crystals within the eutectic regions of the alloy change their shape from highly acicular or needle-like crystals to rough spheroids resembling cubes which have been well-rounded. The degree of spheroidization is dependent upon both the temperature and the duration of the anneal. The limited information available at the start of this investigation indicated that it might be possible to estimate the mean effective temperature to which a specimen of the alloy had been exposed, by a detailed examination of its microstructure after the exposure. The mean effective temperature is that temperature which, if held constant on a test specimen, would produce the same annealing effects in the same length of time on that specimen as were observed on a given sample; the given sample having been annealed at an unknown temperature or unknown temperatures for a specified period of time.

SUMMARY

The response of an eutectic aluminum-silicon alloy to a series of time-temperature anneals has been studied metallographically. Two types of material were investigated; namely, the alloy layer between brazed aluminum components, and a casting of the eutectic alloy. Spheroidizing behavior of the acicular silicon particles in the alloy was determined over the temperature range of 250-550 C (482-1022 F) for periods up to 100 days. A chart depicting the microstructural appearance of the eutectic aluminum-silicon alloy at successive annealing stages is presented. Each annealing stage was assigned an arbitrary number termed the "annealing value". A particular "annealing value" could be attained through a wide variation of time and temperature conditions but for a given "annealing value" only one of these conditions is independent; the choice of one fixes the other.

Thus the "annealing value" can be used to estimate the mean effective temperature to which a sample has been exposed provided the duration of exposure is known. The mean effective temperature is defined as that temperature which, when applied to a test specimen, would produce the same "annealing value" as observed on a given sample, if applied steadily for an equal period of time. An Arrhenius plot of the thermal histories of samples having equal "annealing values" indicated that the spheroidizing of silicon particles is a diffusion-controlled mechanism. The activation energy of the alloy for this process was determined to be 37,700 calories per gram mole for both the braze layer and the cast forms of the alloy.

PURPOSE

The purpose of this investigation was to establish a means of determining the mean effective temperature at which any specimen of Al-Si had been annealed. After the specimen had been annealed, metallographic examination of the microstructure could determine the annealing temperature, provided the duration of anneal is known. This procedure could be used to determine the effective temperature of Al-Si objects in locations normally without temperature indicating or recording devices. This is especially applicable to nuclear reactors wherein each Al-Si-brazed fuel element becomes a temperature recorder. The mean effective temperature for any point of interest could be determined by noting the period of irradiation of a fuel element in that location, then sectioning that fuel element in a Radiometallurgical Facility to obtain the microstructure of the Al-Si-braze layer. The difference between the normal braze material and the relatively pure Al-Si material used as standard process addition alloy was also sought. This would answer the question: Do the impurities picked up during the brazing process affect the annealing behavior of Al-Si?

LITERATURE SURVEY

A substantial amount of work has been done on the nature of internal boundaries in metals, movement of these boundaries, and the measurement of the energies associated with boundary formation, existence, and movement.[2-8] Nucleation of precipitates or second phase particles from

supersaturated solid solutions also has been closely studied.[9-11] However, the study of the later stages of aging, especially when more than one phase is actively involved, has not been covered thoroughly outside of the iron-carbon system. Rosenbaum,[11] when dealing with the aluminum-silicon system, states:

> "A theoretical interpretation of the later stages of aging is complicated by the fact that both plate-like and equi-axed particles are growing, and it is not known whether they change shape during precipitation."

Several articles deal with the problem of nucleation and the rate of nucleation of silicon from supersaturated aluminum-silicon solid solution.[9-12] Two articles deal with the form taken by the silicon phase during solidification as a function of composition of the melt and the cooling rate.[12, 14] However, only one article was found which describes the effects of extended annealing conditions on the structure of Al-Si alloys. Peekema,[1] in his investigations, found that a gradual change occurred in the Al-Si microstructure which would make possible the determination of the mean effective temperature to which a sample had been exposed. The only requirement was that the exposure time had to be known. Peekema also determined the activation energy for the process to be approximately 38,000 calories per gram mole. His work was based on studies over the temperature range from 260 C to 400 C (500-752 F), and used only four points for the determination of the activation energy.

A review of the aluminum-silicon phase diagram (Figure 1) shows a simple eutectic at 12.7 weight percent (w/o) silicon which melts at 577.2 C (1071 F).[15, 16, 17] Casting alloys of aluminum and silicon frequently contain additions of other elements, such as sodium or boron, to control or modify the solidification characteristics.[18] These are called "modified" alloys. Unmodified alloys of this system are usually called normal even though they contain an abnormal eutectic structure. This eutectic structure is considered abnormal because it lacks any apparent order between the two constituent phases. When solidification occurs from an undercooled or supersaturated melt, solidification of the eutectic regions

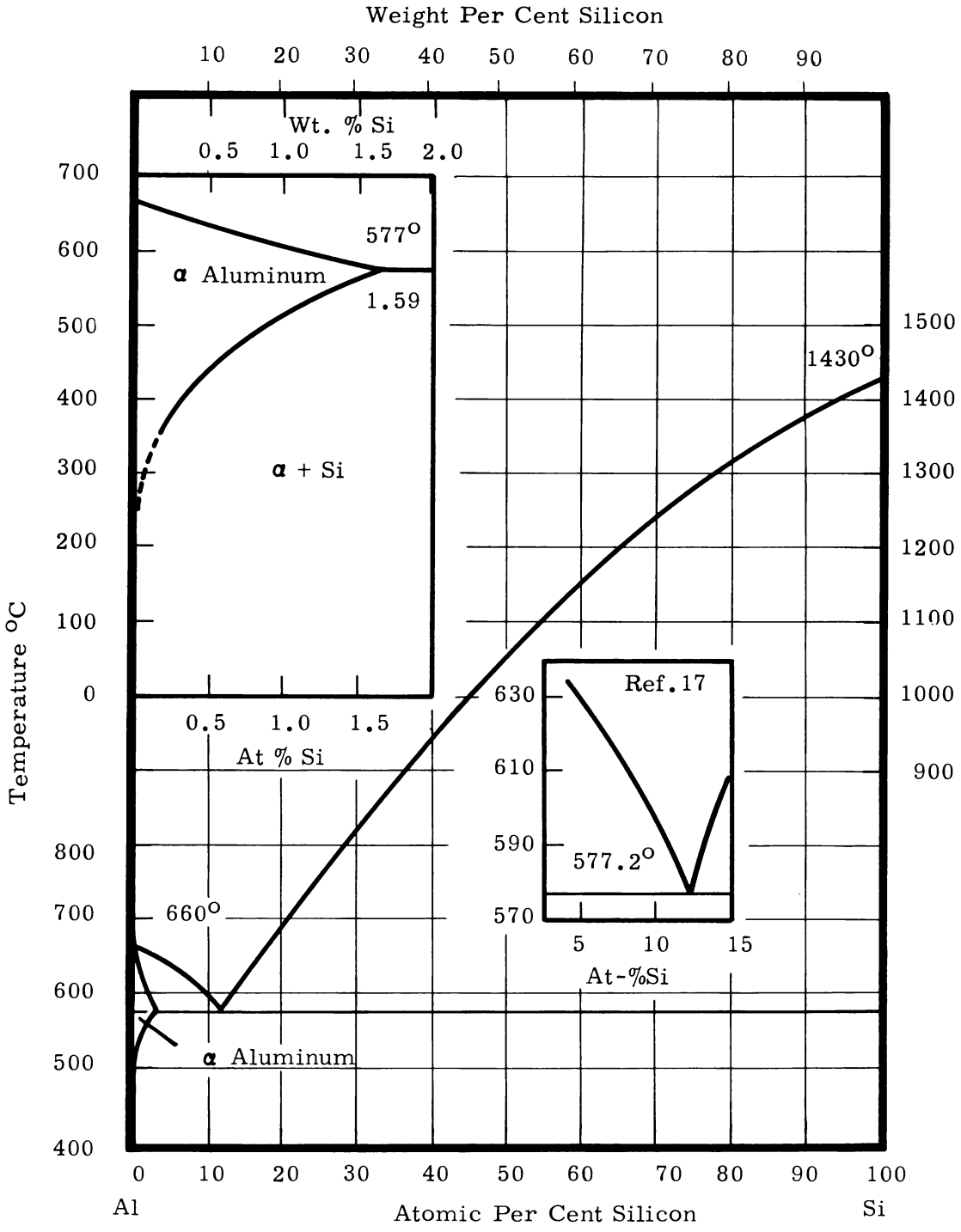

FIGURE 1

Aluminum-Silicon Phase Diagram According to Hansen[15]

AEC-GE RICHLAND, WASH.

is dominated by the growth of silicon platelets in dendritic form in advance of the solidifying matrix of α aluminum.[12]

The aluminum-rich α phase may contain as much as 1.5 w/o silicon in solution at 577 C (1071 F). Rapid quenching of a sample of this composition from 577 C (1071 F) to room temperature will retain all of the silicon in solid solution. The silicon-rich phase will retain some aluminum in solid solution[12] but the amount is so small it is considered essentially pure silicon; therefore, the chemical symbol Si is used to designate this phase.

When the alloy is used as a braze for aluminum components, Al-Si always dissolves some excess aluminum while molten. When the assembled part is quenched, the excess aluminum solidifies first as primary dendrites, saturated with silicon. The remaining eutectic regions then solidify with the Si forming dendrites of interconnected platelets just ahead of the solidifying α matrix.[12] This results in the Si platelets retaining a definite orientation with one another. However the matrix α grains in this same region do not bear any orientation relationship to the Si or to each other although they are bounded and limited by the Si platelets.

EXPERIMENTAL PROCEDURE

Test Material

Aluminum caps from scrapped fuel elements were obtained from the Fuels Preparation Department of the Hanford Atomic Products Operation. These caps contained a braze layer of Al-Si identical in form to the caps removed for sectioning from irradiated fuel elements. Therefore, the results obtained from these caps should be directly applicable, except for the irradiation effect, to the analysis of the thermal history of irradiated fuel elements. Since these caps were taken from a controlled lot of special test assemblies, their composition, thermal history, and texture were essentially the same. The composition of the canning bath was 11.2 w/o silicon, 0.94 w/o iron, 0.16 w/o uranium, 0.24 w/o lead and the balance, aluminum. The aluminum cans were an X-8001 alloy containing 1 w/o nickel. The component parts were assembled at a temperature where the

Al-Si was liquid, then the assembly was quenched into cold water. After various testing programs had been completed, the caps were removed from the fuel elements for use in this study. Each cap was cut into pie-shaped sections, drilled and marked. Each section was drilled to facilitate handling; however, the drill hole was located where it would leave the maximum area available for microstructural analysis. The markings placed on each section identified the specific cap and the section. As many as ten sections were cut from a single cap.

A second group of samples was cut from a one-half inch diameter casting of Al-Si. This was virgin braze material with the composition 11.67 w/o silicon, 0.65 w/o iron, 0.03 w/o nickel, 0.05 w/o chromium, 0.15 w/o lead, 0.03 w/o titanium, and the balance, aluminum. This material had been melted and chill-cast into a graphite mold. The dendritic form of the Si was much more evident and much larger in this Al-Si casting than it was in the braze layers of the caps. These were also cut into small sections with a hole drilled in the center of each.

At least one section from each cap and two sections from the Al-Si casting were polished for microscopic examination in the nonheat-treated condition. In all cases, the primary aluminum dendrites were found to contain no precipitated Si which could be resolved with the optical microscope. The primary Si grains took any of several forms as shown in the nonheat-treated portion of the chart used to establish annealing values.

Heat Treatment Schedule

The schedule for the heat treatment of the specimens was evolved from data provided by Peekema.[1] His preliminary work provided data on 28 separate samples which had been exposed to temperatures between 260 C and 400 C (500 F to 752 F) for periods up to 80 days. A portion of these samples had not been annealed sufficiently to cause a recognizable change in microstructure. Extrapolation of Peekema's results established a region of probable results and of major interest. A variation of the Arrhenius plot was used to analyze Peekema's results and the same method of plotting was used for planning and analyzing purposes by

the author. The plot of all known data from Peekema's work and other sources is shown in Figure 2. The zone chosen for detailed study is outlined on Figure 2. It extends from 1/100 of one day to 100 days and from 250 C to 550 C (482 F to 1022 F). Those points to the right and below the zone chosen would not show sufficient annealing effect to be of any value. The sloped line at the top left of the zone in Figure 2 was above the time-temperature exposures expected to be encountered. These two areas were left out of the study for these reasons.

The region of intended investigation was divided into nine temperature and nine time steps to give equally spaced points on the Arrhenius plot. These values are given in Table I. One group of samples, Series A, was divided so that all of the samples for one temperature were cut from one cap. A cross-check was made by heat-treating all samples cut from another cap according to conditions indicated by lines of equal annealing effect as predicted from the preliminary data. This second group of samples became Series B.

A third group of samples, Series C, consisted of sections of the chill-cast virgin Al-Si. This group was assigned positions across the middle of the region of interest in a broad band parallel to the predicted slope of lines of equal annealing effect. The plotted positions of these three groups can be easily seen in Figures 8, 9 and 10 in Appendix B, where the results of the anneals are reported in simplified chart form.

Standards were needed for comparison of results. To obtain standards at intervals close enough to eliminate ambiguity, extra samples were added to Series A at two temperatures. The extra samples were annealed at 275 C and 404 C (527 F and 759 F) at times midway between the times (on the Arrhenius plot) for the balance of the samples. The groups of samples at these two temperatures then had a time spacing on the Arrhenius plot of exactly one-half that of the balance of the specimens.

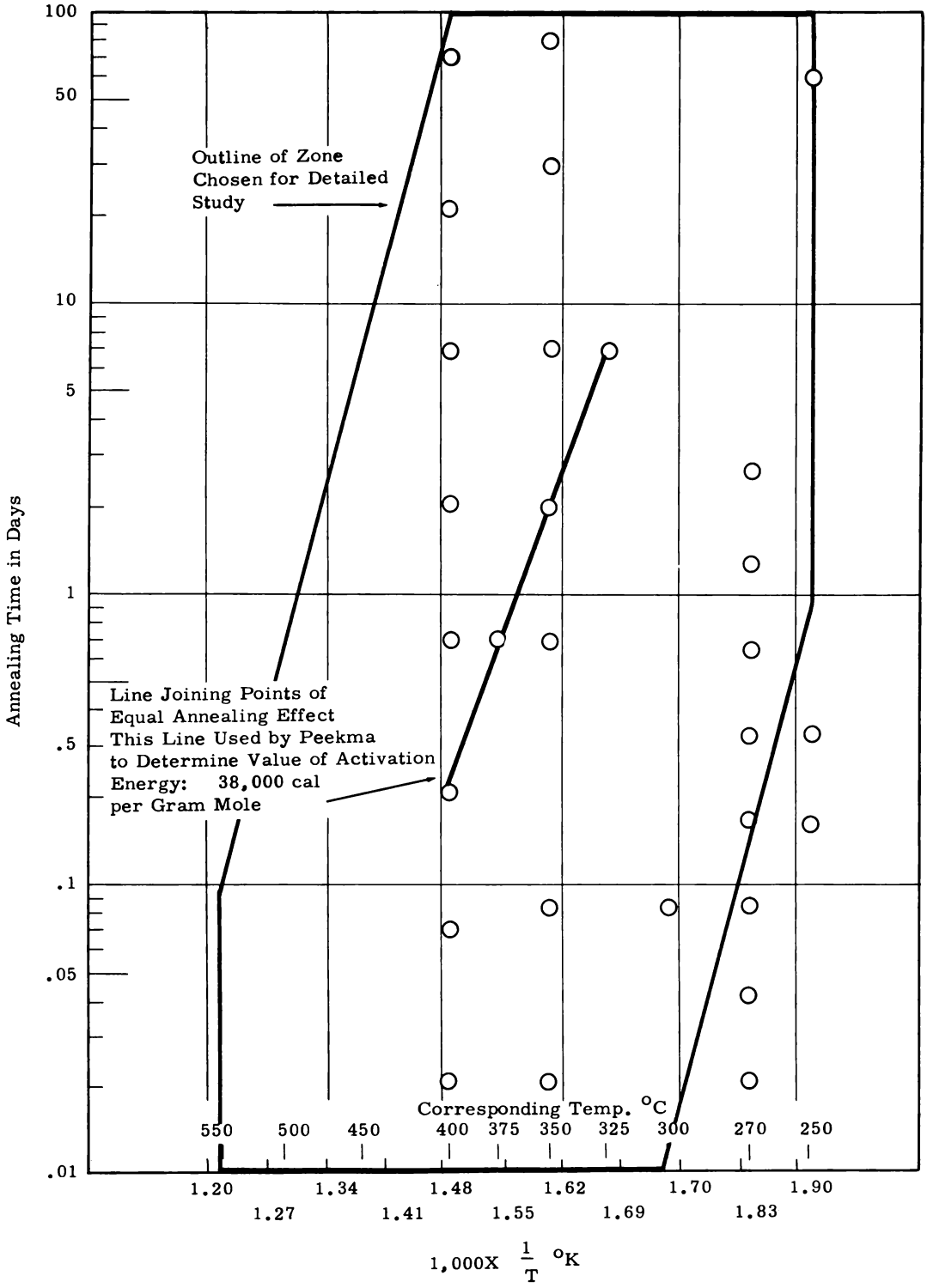

FIGURE 2

An Arrhenius Type Plot of the Time-Temperature Conditions for Al-Si Samples Annealed Prior to This Study

AEC-GE RICHLAND, WASH.

TABLE I

DIVISIONS MADE IN TEMPERATURE AND TIME TO GIVE VALUES EVENLY SEPARATED ON ARRHENIUS PLOT

Temperature Divisions		Time Divisions		Extra Time Divisions for Standards	
$\frac{1000}{T\ ^{o}K}$	^{o}C	$Log_{10}\ t$	t in days	$Log_{10}\ t$	t in days
1.2151	550	-2.00	0.010	.	.
1.3022	495	-1.50	0.0316	-1.75	0.0178
1.3893	447	-1.00	0.100	-1.25	0.056
1.4764	404	-0.50	0.316	-0.75	0.178
1.5635	367	0.00	1.00	-0.25	0.562
1.6506	333	+0.50	3.16	+0.25	1.78
1.7377	303	+1.00	10.0	+0.75	5.62
1.8248	275	+1.50	31.6	+1.25	17.8
1.9119	250	+2.00	100.0	+1.75	56.2

A computational error was made early in the experimental program; before it was discovered several samples had been annealed at incorrect temperatures. When the error was discovered it was decided to incorporate these samples into the study since the temperatures fell between those desired. These samples are included in the statistical analysis but are not shown in the simplified plots, Figures 8, 9 and 10 of Appendix B, because of the difficulty of adding them to such a plot.

Annealing Procedure

All samples were marked and designated for a particular heat treatment. All those destined for the same heat treatment were wired together with clean iron wire. An electrically heated muffle type furnace was used for the first few heat treatments. This unit performed satisfactorily for short periods of time but could not be used for the long-term anneals.

Extended anneals were carried out in a bank of six Marshall tube furnaces. A Weston Electric Instrument Corporation Celect-Ray six-point controller was used to control the furnaces at six different temperatures. Furnace temperatures were monitored with a six-channel Brown recorder. The Brown recorder contained an override feature which could be set to turn off any furnace should the indicating thermocouple exceed the desired temperature by 5 C.

The Marshall tube furnaces were lined with a quartz tube closed at one end. Fibrofrax furnace insulation was used to caulk the small opening between the end of the furnace proper and the quartz tube. Failure to caulk this opening could result in 5-10 C variation of sample temperatures as the furnace room air circulation pattern changed during the day. While testing these furnaces for reliability it was possible to tell the exact minute the furnace room door was opened in the morning by reviewing the recorded temperatures on the Brown recorder. For furnace testing, a thermocouple was ballasted with a spare sample clamped onto the bead. This assembly was placed in the furnace to be tested, and wired into the Brown recorder point for that furnace. To check the variation of temperature within a furnace the ballasted thermocouple was moved from one position to another in the central hot zone of the furnace.

In the initial furnace assembly, using only the quartz tube, closed at one end and capped at the other, temperature variations in excess of 20 C were measured in the central zone. Fluctuations of temperature at a single point were noted to be more than 10 C as the furnace current was cycled off and on by the controller.

The final furnace assembly consisted of the quartz tube inserted into the furnace and caulked between the tube and furnace to prevent free air movement. Fibrofrax was packed into the quartz tube from the closed end to the central zone and on the other side of the central zone to the open end of the tube. The central zone was occupied by a six-inch, U-shaped boat made of one-quarter inch aluminum plate wrapped with four layers of bright aluminum foil. The high reflectivity of the aluminum tended to flatten

out and equalize radiation heating effects. Fluctuations of temperature were cut down by the ballasting effect of the rather large amount of aluminum present and the high heat capacity of the aluminum. The high conductivity and thick section of the aluminum boat further equalized the temperatures in the central region. Aluminum foil reflectors were placed at both ends of the central section, both to help contain the radiant heat and to keep the furnace insulation out of that section. The central section then contained a space six inches long by one and one-half inches in diameter surrounded by aluminum ballast and aluminum reflectors. Each of the six furnaces was assembled in like manner. The recording thermocouple was placed in the end of the U-shaped boat by drilling a hole one-half inch in from the end and peening the aluminum about the thermocouple placed in this hole to insure positive thermal contact.

Temperature tests with the ballasted test thermocouple revealed no detectable fluctuation as the furnace current cycled on and off. A variation of about 1 C existed along the six-inch length of the central zone at 404 C (759 F). Less than 2 C variation existed between the readings of the recording thermocouple and the ballasted test thermocouple. The greatest temperature fluctuations were caused by fluctuations in the standard carbon cell in the Celect-Ray controller. Further discussion on this point may be found in Appendix A.

Actual heating times for samples placed in these furnaces were found to be approximately seven minutes. Samples for the longer time anneals were assumed to require negligible heating time. Where this heating time of seven minutes was more than one per cent of the total time, as for anneals of less than half a day, a liquid metal contact was used for rapid heating. At the higher temperatures pure lead was used; and at temperatures below the melting point of lead (327 C) (621 F) Wood's metal was used. A piece of the low melting metal was placed on the aluminum ballast in an otherwise empty furnace (meaning no samples) where it was allowed to melt and come up to furnace temperature. When the furnace had stabilized, the samples for short-term anneals were placed in the liquid metal and the furnace was closed. Approximately two and one-half

minutes were required to heat a sample to furnace temperature by this method. This time was added to the annealing time. As each sample was withdrawn from a furnace, it was quenched into water, both for ease of handling and to terminate the annealing period.

A test was run on two Al-Si samples to determine the effect, if any, of heating Al-Si in contact with lead. This test is described in Appendix A and illustrated in Figure 6. It was concluded that heating samples in contact with lead for short periods would have no significant effect on the spheroidization characteristics of the Si phase in Al-Si.

Metallographic Preparation of Samples

All of the samples were prepared in one of the following two ways. Each sample was mounted in transparent cold setting plastic. The plastic used bears the trade name of Thalco Resin. Mounted samples were ground on a wet belt sander, then hand processed through successively finer grades of silicon carbide abrasive papers ending with the 600 grade. The final grinding was done on 3/0 French emery paper. A few of the samples were polished by hand through six micron diamond paste on Microcloth, using filtered kerosene as lubricant on an eight-inch, high-speed wheel, followed with magnesium oxide powder on Gamal cloth with distilled water on an eight-inch, low-speed wheel. Samples of low degrees of annealing value were polished easily by the hand method but the samples of higher annealing value were more and more difficult to polish. Finally it was decided to polish all of the remaining samples in the Syntron viratory polishing bowls.

For vibratory polishing the procedure was the same through the step producing a good 3/0 finish on the sample. At this point the sample was weighted and placed in a 12-inch bowl of the Syntron vibratory polishing unit. This bowl contained Gamal cloth cemented firmly to the bottom, magnesium oxide polishing powder, and distilled water. It was essential to start with the entire assembly cold, to prevent deterioration of the magnesium oxide abrasive. As the bowl was warmed by the operation of the machine, the abrasive became slimy to the touch and very ineffective.

This deterioration of the abrasive is probably due to hydrolysis of the magnesium oxide, and low temperatures retard the reaction.

Complete polishing of the samples was usually accomplished within about two hours. Fifteen to twenty samples were loaded at one time and three to five of these usually required more polishing or even regrinding. About as many more needed a final touchup polish on the hand lap. Approximately half a normal charge of samples finished the vibratory polishing step with a significantly better finish than could be attained by hand polishing. After annealing, these samples were extremely soft and smearable. In fact, they were so soft that the metallographer's main concern was to polish the samples with any means available. Economy of labor was not the criterion; however the use of the Syntron vibratory polishing units did save many manhours. On the more difficult samples the author performed all of the metallography.

Each sample was etched by swabbing with one-half percent hydrofluoric acid for about ten seconds. This etch cleaned the sample of smeared metal and accentuated the normal difference in appearance between the aluminum matrix and the Si phase. The grain boundaries of neither the aluminum nor the Si were delineated.

A single photomicrograph at 750 diameters was taken of each sample. The entire sample would be scanned and a representative area photographed. In a few cases where a single view was not descriptive of the entire sample, additional photomicrographs were taken.

DISCUSSION OF RESULTS

When annealed at sufficiently high temperatures the Si platelets begin to spheroidize. The degree of spheroidization depends on both the temperature and the time of annealing. Spheroidization of the Si can be compared to grain coarsening in other metals. However, in this system, the individual Si particles are separated by a second phase, the aluminum, in contrast to most grain coarsening experiments which have dealt with single phase materials.[4-8, 19] In the Al-Si system the existing Si crystals

spheroidize by rounding of the platelet edges and by breaking down the platelets into smaller, thicker particles of lower surface energy. Any excess silicon in solid solution in the matrix α phase is deposited on the nearest particle of Si. As some of the particles reach relative crystalline perfection they begin to grow by drawing silicon from their more imperfect neighbors by a process of dissolution, diffusion, and deposition..

In the more common single phase systems grain coarsening proceeds in much the same manner. The more perfect grains grow at the expense of their imperfect neighbors by a process of dissolution and deposition. By comparison the intermediate step of diffusion is very nearly, if not entirely, missing because the grain boundary is advancing with the growing grain and transport of material is unnecessary; only an atomic rearrangement at the grain boundary is required. Also, in a single phase material, there is a practical limit to the size attainable by a given grain because of impingement of that grain upon equally perfect neighbors. This maximum size effect is not reached or even approached in the Al-Si system because of its two-phase character.

Originally the Si platelets are joined in dendrites; they are uniform in cross-section and all of those of a particular dendrite have a definite orientation toward each other. On initial exposure to annealing temperatures several things begin to happen. These changes can be followed on the Annealing Number Charts in Figure 3. In the eutectic regions the excess silicon held in solid solution in the matrix α aluminum precipitates out on the existing Si platelets. This produces a myriad of uneven lumps on the otherwise smooth platelets. These Si platelets begin to coalesce and round off their edges; to become thicker in some places and to become thinner in others. Each platelet separates into pieces which are nearly equi-axed in dimensions. The thinner platelets accomplish this change first and the thicker platelets last. The thickest platelet that has just broken into smaller segments is an indicator of what annealing stage the sample is in. A striking characteristic found on some Si platelets is the tendency for the platelet to change in cross-section from a smooth needle to a ladder-like arrangement

of incomplete three-sided squares. On further annealing each segment separates from the rest and turns in on itself by completing the fourth side of the square.

While the platelets are breaking up as described above, the primary α grains are also changing. Even after the shortest anneal, the nucleating grains of Si within the α grains can be seen under the optical microscope as small dots. These have the appearance of very fine pepper on the Annealing Charts (Figure 3). Further annealing initially causes a greater number of nucleation sites to appear; those appearing first grow rapidly and soon begin to swallow up their smaller neighbors. As growth continues, a band appears next to the edge of the α primary grains which does not contain any of these secondary crystals of Si. Careful study will show the nearby eutectic zone Si crystals are larger than similar crystals farther from the primary α grain. These crystals have become larger by absorbing the secondary silicon in the band at the edge of the α grain. As annealing proceeds, this band, free of secondary Si, grows wider until at an Annealing Number near 22, the primary α grains are once again free of all Si crystallites within their boundaries. Secondary precipitation of Si within the primary α aluminum grains thus becomes another important indicator of the degree of the anneal. The secondary Si does have this drawback as an indicator: at higher temperatures of anneal, more silicon can remain in solid solution, and less will be available for precipitation as secondary crystals. Thus a sample annealed at high temperature may have the same annealing value as a sample annealed for a much longer time at lower temperature; but the appearance of the secondary Si crystals within the primary α grains will be distinctly different. The secondary Si crystals will disappear first from the sample of higher temperature anneal.

MEASUREMENT OF RESULTS

Measurement of the degree of annealing posed a serious problem for the Al-Si system. An oversimplified statement of this problem would be: Measure the increase in grain size of the grains of the Si phase with corresponding increases in annealing exposure. Nearly all of the grain size measuring methods in use are designed to be used on equi-axed grains

in single phase material.[4-8, 19, 20] What was needed here was a method of determining the degree of change of the Si crystals regardless of changes of melt composition, impurity content, and initial size of these crystals.

All of the conventional methods for establishing absolute grain size were tried but without success. A discussion of these methods is in Appendix A. A workable arbitrary system of standards was set up as follows: Two sets of samples had been heat-treated for various time intervals at the temperatures of 275 C and 404 C (527 and 759 F). Photomicrographs of these 32 samples were assembled in the order of increasing heat treatment. The series for the two temperatures were compared visually and were found to overlap. A good overlap fit was made and the photomicrographs were numbered consecutively from 1 through 30, representing the least heat treatment as number 1 and the most extensive heat treatment as number 30. These numbers were designated by the name Annealing Value. All photomicrographs had been taken at the same magnification - 750 diameters. The photomicrographs for the balance of the samples were now compared with the arbitrary standards and each in turn was assigned an annealing value number.

After about one-third of the photomicrographs had been processed it became apparent that something was wrong with the sequence of the arbitrary standards. Also, one picture was being used to compare with many, and the basic structures of the many differed sharply from the one. For a better understanding of what this difficulty was, the author laid out all of the graded photomicrographs on a large table according to their assigned Annealing Values. With a large number of photomicrographs displayed, it became apparent that there were a variety of basic structures in the initial lot of samples. These basic structures in the initial lot of samples varied from extremely fine, barely resolvable masses of Si crystals, through an open structure of intermediate sized Si crystals, to very acicular, strongly dendritic Si crystals with wide spaces of α aluminum between the Si crystals. All of these structures, illustrated on Figure 5 in Appendix A, were found in the eutectic regions where excess aluminum had already

diffused to the primary α grains, leaving these eutectic regions essentially stoichiometric. The graded photomicrographs, already arranged according to Annealing Values, were then further sorted according to basic structure.

At this point it was decided to double check the Annealing Value so arbitrarily assigned to the "standard" photomicrographs. These pictures were removed, leaving the balance in place on the table. The "standard" pictures were shuffled as one would shuffle a deck of cards. Then, without reference to the identifying marks on the back of the pictures, the "standard" pictures were assigned Annealing Values according to the array remaining on the table. All but a few of the "standard" pictures were reassigned to their original Annealing Values. A close study of those that did not fit resulted in removal of two standard numbers and recognition of anomalies existing in the standard sample series at three different places. This action reduced the number of standard Annealing Values to 28. The anomalies can be seen in the simplified plot of results given in Figure 8 of Appendix B.

The "standard" photomicrographs having been rechecked, the rest of the photomicrographs were also rechecked. Everything except the standard pictures was removed from the display table and shuffled thoroughly. All of the pictures not yet graded were also shuffled into the stack. Each picture was assigned to a place on the display table according to basic structure and Annealing Value. As the number of pictures displayed increased it became progressively easier to determine the proper location of each new picture. At this time it became apparent that any standard chart of Annealing Values must contain examples of the various basic Al-Si structures at each Annealing Value.

After all the pictures were displayed on one table, without reference to the identification numbers on the back of each print, the entire array was criticality reviewed. When all the prints were assigned to the proper Annealing Value and basic structure group, the prints were turned over and the sample number from each print was recorded with its proper Annealing Value. These values are recorded in Table IV of Appendix B. Figures 8, 9 and 10 of Appendix B show a simplified plot of these values according to annealing conditions.

Figure 3 is composed of the "standard" photomicrographs and an example of each type of structure under each Annealing Value. Some particular structural combinations were not available for this chart because none were found during this study. A set of nine photomicrographs is shown in Figure 3 to illustrate the many variations of structure obtained in the nonheat-treated samples.

A very fine separation exists between the structures of each of the Annealing Values. If the sample identification were known, it would be quite easy to allow the visually determined estimate of Annealing Value to slide two or even three units to one extreme or the other in order to place it into a preconceived relationship with other samples. For this reason no re-evaluations were made. It was felt that any re-evaluation must be done in such a manner that the identity of the subject sample was hidden from the evaluator. Although there were some obvious errors in the lower range of Annealing Values, these errors were felt to be unbiased and as such should cancel out in a statistical analysis. In the upper range of Annealing Values evaluations were much simpler and fewer errors occurred.

It is the author's opinion that Annealing Values below fifteen should be held suspect because there are insufficient structural differences in this area to permit a reliable estimate of Annealing Value. If sufficient data can be made available to conduct a statistical analysis, values below fifteen become meaningful. Annealing Values above fifteen should be reliable whenever the evaluator can make an unbiased estimate. Probable error in this region should be within one Annealing Value unit.

There is more chance for error in the selecting and taking of photomicrographs than in evaluating them. This is due to initial microstructural differences which introduce a consistent bias in evaluation. This is shown by comparing the final Annealing Values of the samples of Series C with those of Series A and B. The casting of Al-Si, from which the samples of Series C were cut, contained a coarse acicular, and very open grain pattern as contrasted to the structure of Series A and B. In Figures 8, 9 and 10 of Appendix B the average positions of lines of equal Annealing Value shift to

the left for the Series C samples as compared to both Series A and B. This shift amounts to approximately one position difference on this simplified Arrhenius plot. Similar shifts were noted for those samples of Series A and B possessing large acicular grains of Si. Because of this variation an evaluation of a single sample should be based on photomicrographs sufficient in number to cover all variations of basic structure within the sample. By evaluating each photomicrograph and averaging the results, a more accurate estimate of the Annealing Value of that sample can be made.

The reproducibility in using the chart (Figure 3) for determining Annealing Values was tested in the following manner: Two colleagues of the author were briefed on the microstructural changes which occur in the Al-Si system during annealing. Then they were given photomicrographs previously graded by the author and asked to make their own determination according to the Annealing Value chart. The first two or three prints were duplicates of those used in the chart. When they had located the duplicate prints, they tried their skill at evaluating about a dozen additional photomicrographs. In each case the first few evaluations were made with much hesitancy and deliberation. As the test proceeded proficiency increased rapidly. The final score listed one sample three units off the author's predetermined value, about six were off by two units to either side of the author's value, and the balance either agreed with the author's value or were only one unit off to either side. Since experience rapidly increases proficiency, it was felt by all three persons involved that a metallographer working with this material could probably duplicate the results of a given problem with an accuracy of plus or minus one Annealing Value unit with only an occasional two-unit error.

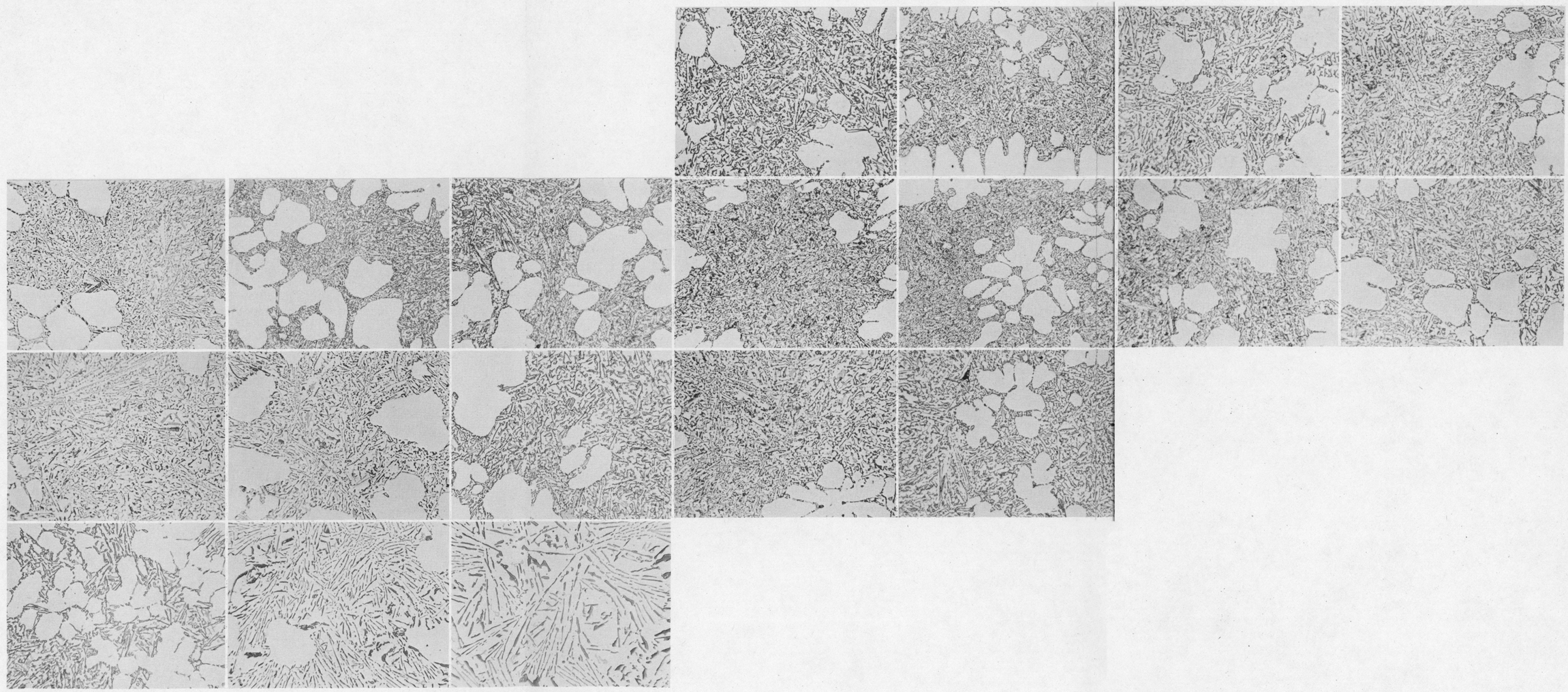

FIGURE 3

A Comparative Chart Showing the Progressive Stages of Spheroidization of the Si Phase in Al-Si Samples. The Degree of Spheroidization is Represented by the Annealing Number. Original Magnification 750 X. Reproduced at 500 X.

AEC-GE RICHLAND, WASH.

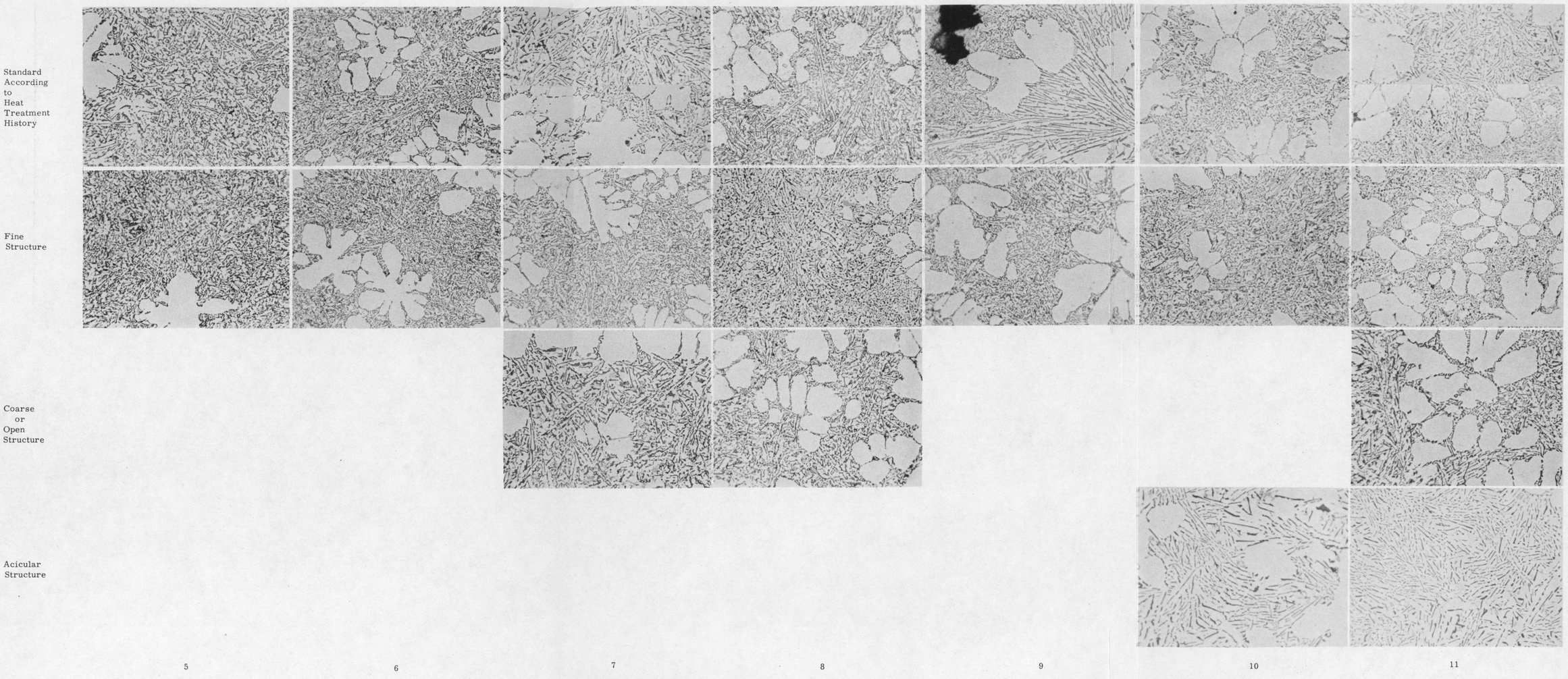

FIGURE 3 (Continued)

AEC-GE RICHLAND, WASH.

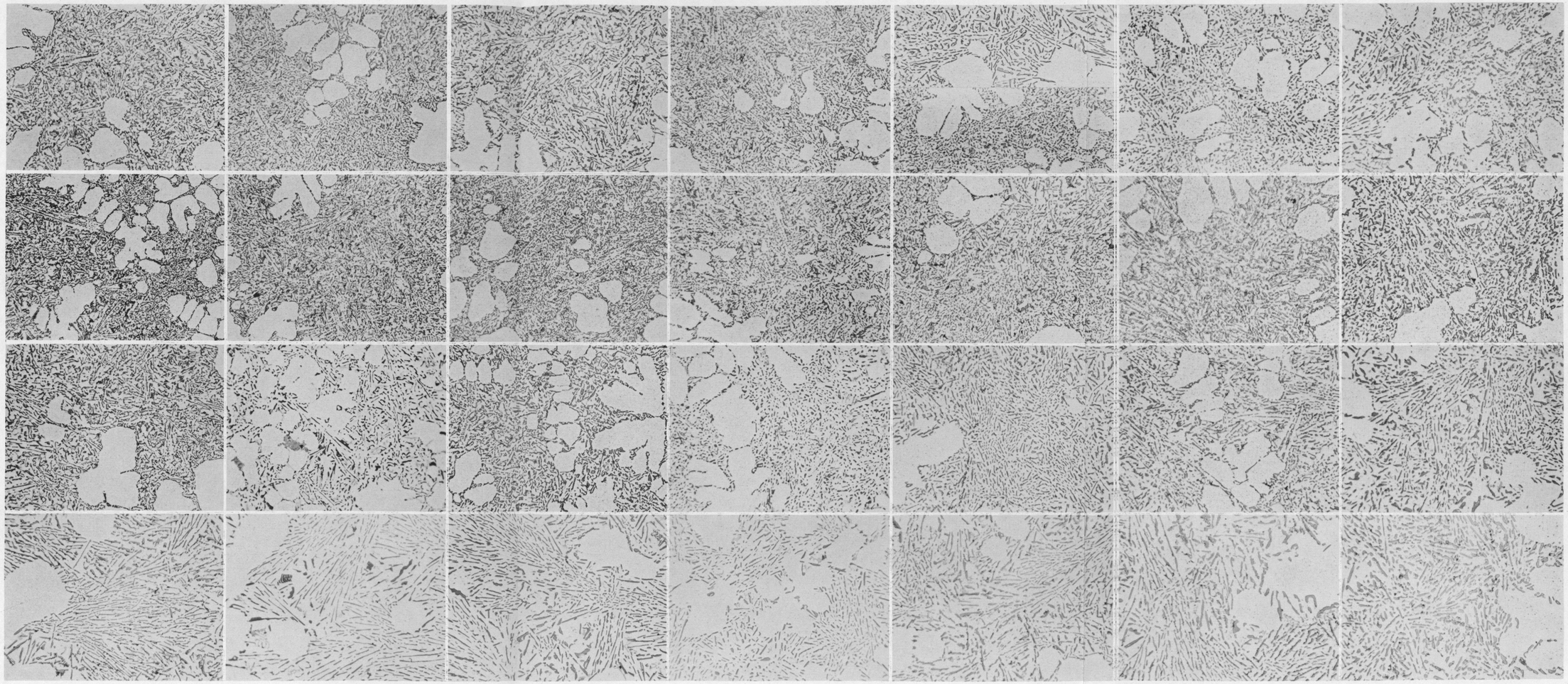

FIGURE 3 (Continued)

AEC-GE RICHLAND, WASH.

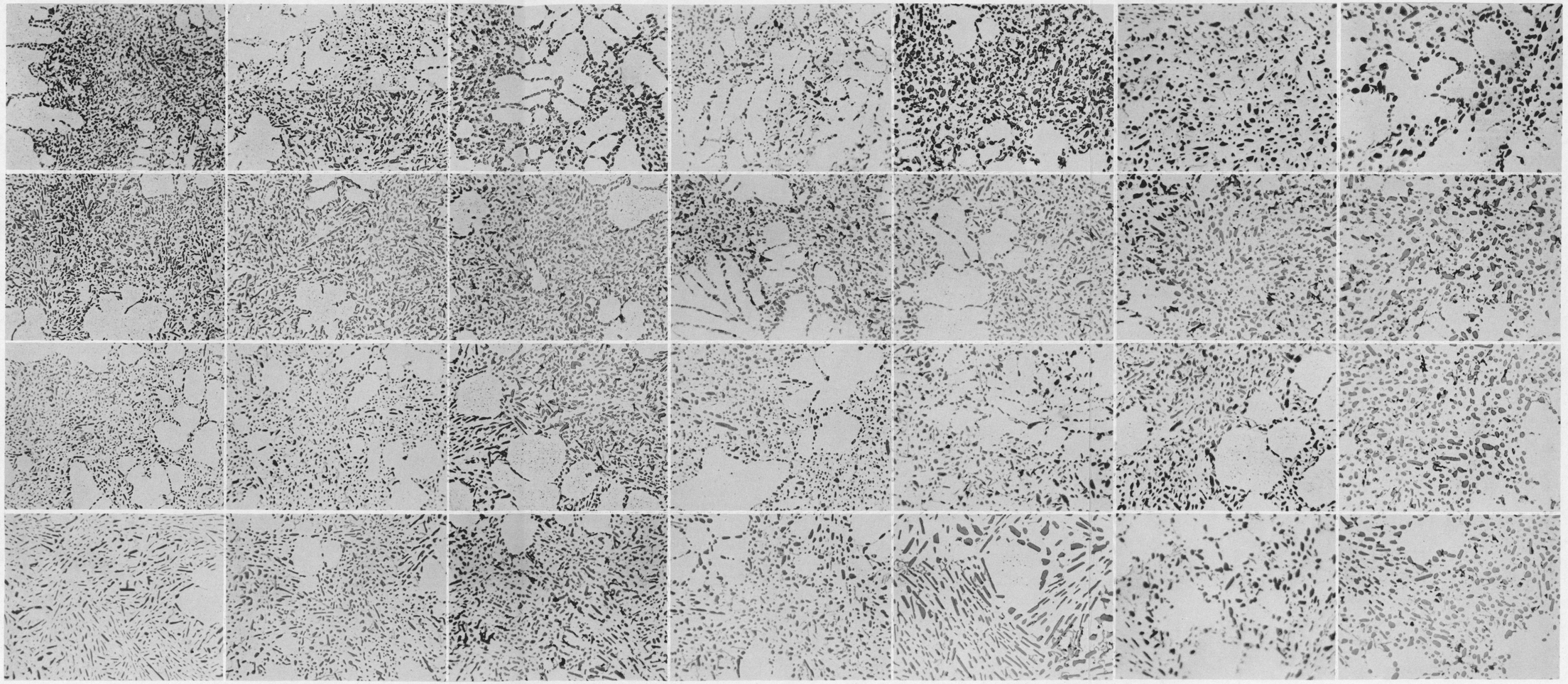

FIGURE 3 (Continued)

AEC-GE RICHLAND, WASH.

Standard According to Heat Treatment History

Fine Structure

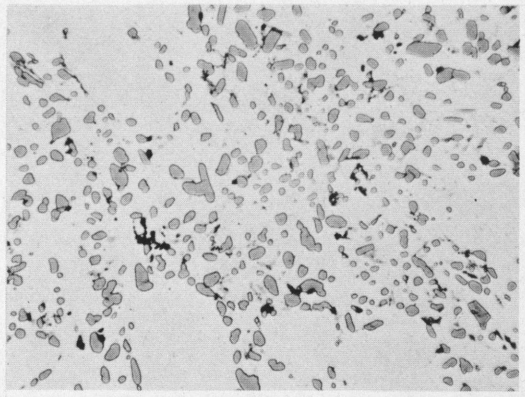

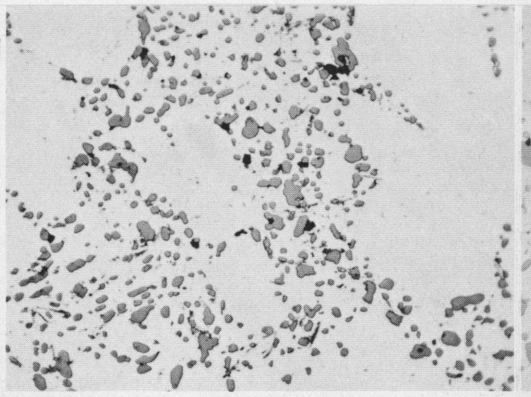

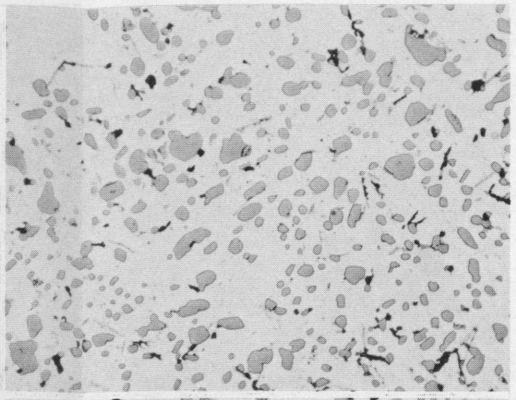

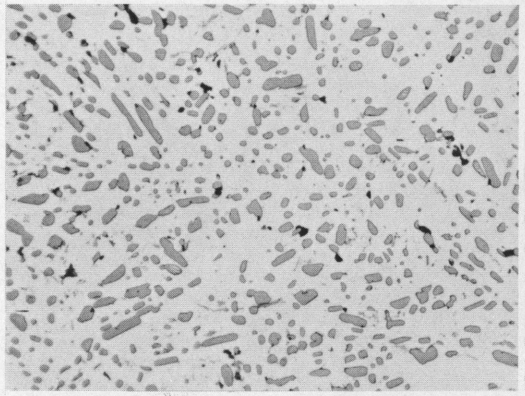

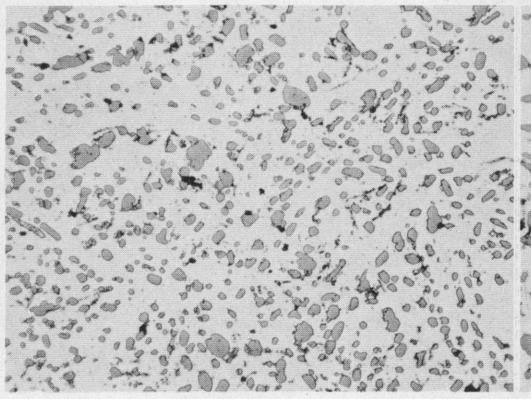

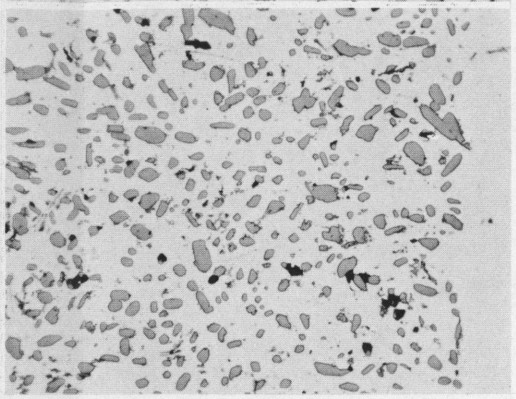

Coarse or Open Structure

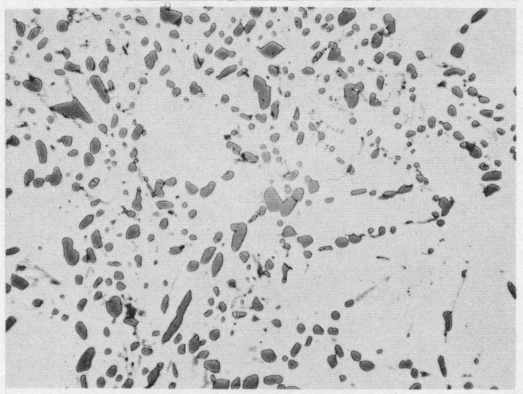

Acicular Structure

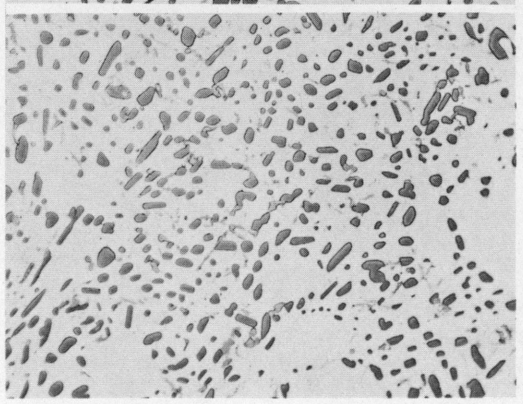

26 27 28

FIGURE 3 (Continued)

AEC-GE RICHLAND, WASH.

MATHEMATICAL ANALYSIS

This entire annealing program was developed in conjunction with a statistician to ensure the data obtained would have maximum statistical value. When the Annealing Values of all samples were available, they were presented to the statistician for analysis. A regressive analysis was conducted which established values for a mathematical function of the form $\frac{1000}{T} = A_N + b \log_{10} t$ where T is temperature in degrees Kelvin, t is annealing time in days, A_N is the graphical intercept value and is dependent upon N, the Annealing Value number, and b is the slope of the Arrhenius plot. From the value found for b (0.1215) the activation energy for the process is established as 37,700 calories per gram mole. The dependence of the intercept, A_N, on the value of N was found to follow the relationship $A_N = 1.9675 - 0.01821N - 0.00026N^2$. Additional information on the mathematics involved can be found in Appendix B.

GENERAL DISCUSSION

The fit obtained by the regression analysis is shown in Figure 4 for three values of N. The intercept point for each of these lines (at one day where $\log_{10} t = 0$) was calculated from the formula given above, and the slope, b, has the value 0.1215 as given above. Each dot on the chart, Figure 4, represents one condition of heat treatment. Each sample with an Annealing Value equal to that of the plotted line is indicated by appropriate encirclement. A broken or dashed encirclement indicates an interpolated value. Interpolated values were used on this figure, where the raw data indicated they were reliable, to increase the amount of data available for direct comparison with the plotted lines. Interpolated values were not used for any other part of this analysis.

From this comparison of raw data versus plotted formulae, the degree of probable error in establishing the proper annealing value of a sample becomes apparent. For the value N = 8, the maximum variation shown amounts to slightly over one spacing on the chart, or two Annealing Value units. For the value N = 14, a similar maximum error exists. There are twelve positive points and two interpolated points shown for

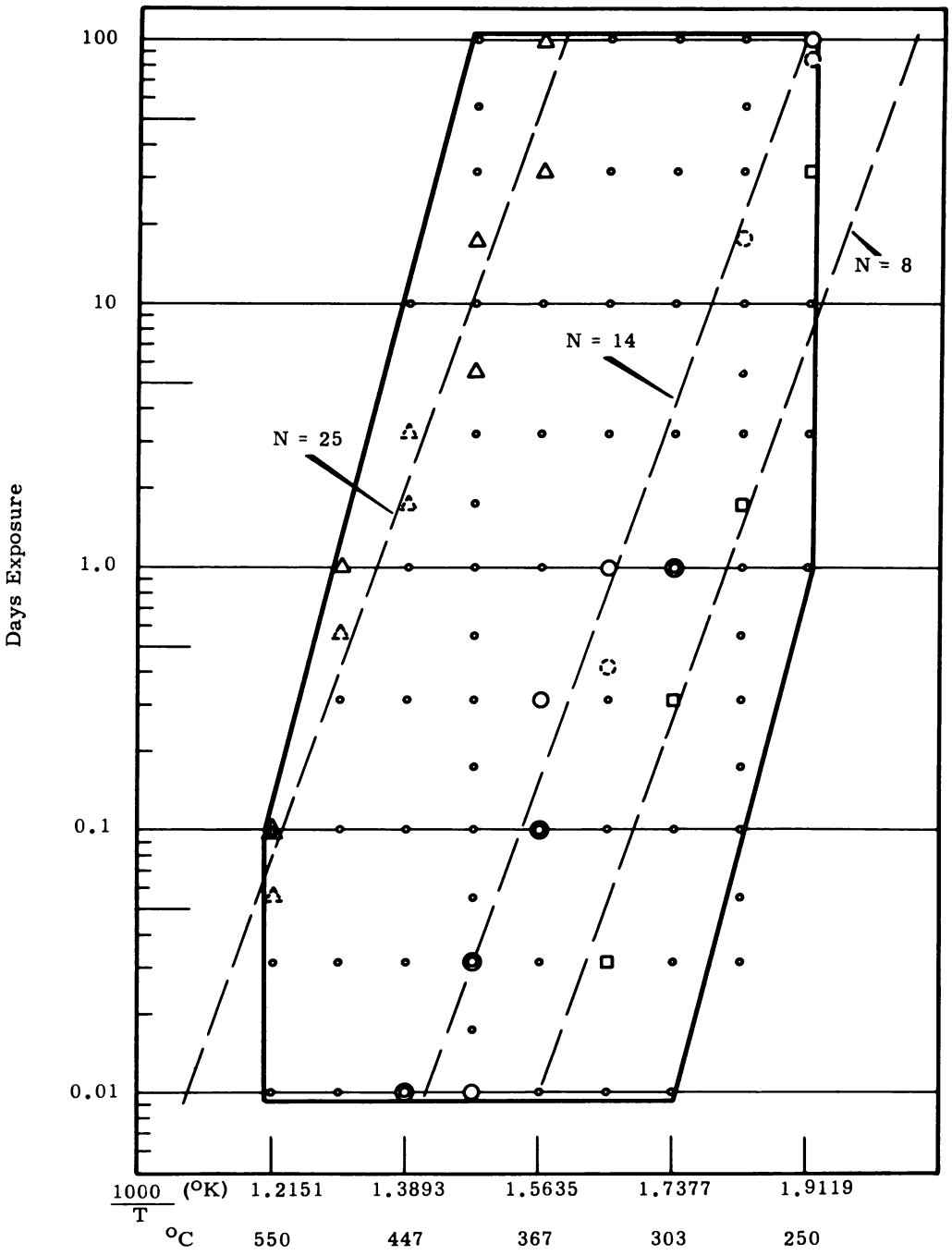

FIGURE 4

Comparison of Raw Data with Calculated Lines of Equal Annealing Value. The Fit of These Lines with Actual Data Points is Shown by Appropriate Encirclement of Points Representing Annealing Conditions. Points with an Annealing Value of 25 are Designated by Triangles; Annealing Value of 14 by Circles; and Annealing Value of 8 by Squares. Broken Symbols Indicate Interpolated Data Points.

AEC-GE RICHLAND, WASH.

N = 14 versus only four positive points shown for N = 8. Two points miss the plotted line of N = 14 by two Annealing Value units while one of the four points for N = 8 is off to a like degree. This would indicate a two-fold increase of probable accuracy for the Annealing Value 14 range as compared to the Annealing Value 8 range. By itself the presentation in Figure 4 cannot support such a conclusion, but when the array of data in Figures 8, 9 and 10 of Appendix B is considered, this conclusion appears quite valid.

When a similar study is made of the N = 25 line on Figure 4, two points are found which are off the line slightly more than one Annealing Value unit but less than two units. This indicates a further increase of reliability at the higher Annealing Values. The cumulative errors in Annealing Values correspond to a temperature error of approximately ± 30 C.

CONCLUSIONS

Estimation of the mean effective temperature to which a sample of Al-Si has been exposed for a definite period of time can be made by careful examination of its microstructure. Accuracy of this estimation is within the range of plus or minus 30 C in the range tested (250-550 C) (482-1022 F).

An appreciable error can be introduced due to variations in original microstructure. A coarse, acicular structure will generally result in determinations on the high side of the range given above. Another contributing factor to error is the selection of an area for the test photomicrograph. If a sample has nonuniform microstructure, better results can be obtained by taking a series of photomicrographs and averaging the results obtained from each.

Standard methods of measuring grain sizes do not apply to the Si crystals in Al-Si. Comparative grain size measurements at low magnification are not of any value for this type of study. At the magnification required for study of annealing effects (500 to 750 diameters) the only successful method found for measurement of the annealing effects was a comparison chart set up on an arbitrary scale.

Grain size of the Si crystals in Al-Si is not a criterion of the annealing effect incurred. Manifestations of annealing are displayed in the microstructure of Al-Si by secondary precipitation of Si in the primary α dendrites, subdividing of thin Si platelets, coalescence of Si crystals, and general spheroidization of Si crystals.

Activation energy required for the spheroidization process of Si crystals in Al-Si is 37,700 calories per gram mole.

The impurities picked up during the brazing process of fuel elements do not affect the annealing behavior of Al-Si beyond that induced by the reduction of the size of the crystals of Si in the eutectic regions. The actual change of annealing effect is negligible; but the change in Si crystal size introduces a bias whereby the apparent annealing effect is lowered.

ACKNOWLEDGMENTS

The writer is deeply grateful for the co-operation of L. A. Hartcorn and the technicians of the Metallography Laboratory whose expert assistance made this study possible.

Gratitude is expressed to S. H. Bush for his suggestions and patient guidance throughout this work; to J. C. Tverberg and D. L. Gray for their encouragement and willing assistance; and to W. L. Nicholson for statistical assistance in planning and analysis.

REFERENCES

1. Peekema, R. M. "Spheroidization of Acicular Silicon in Aluminum-Silicon Eutectic Alloy," Unpublished, June, 1956.
2. Betcherman, I. I. "Rate Processes in Physical Metallurgy," Progress in Metal Physics, 2: 53-89. New York: Interscience Publishers, Inc., 1950.
3. Darken, L. S. and R. W. Gurry. Physical Chemistry of Metals. New York: McGraw-Hill, 1953.
4. Smith, C. S. "Grain Shapes and Other Metallurgical Applications of Topology," Metal Interfaces. Cleveland: American Society for Metals, 1952.
5. Fullman, R. L. "Boundary Migration During Grain Growth," Metal Interfaces. Cleveland: American Society for Metals, 1952.
6. Beck, P. A. "Interface Migration in Recrystallization," Metal Interfaces. Cleveland: American Society for Metals, 1952.
7. Burke, F. E. and D. Turnbull. "Recrystallization and Grain Growth," Progress in Metal Physics, 3: 220. New York: Interscience Publishers, Inc., 1952.
8. Chalmers, B. "Structure of Crystal Boundaries," Progress in Metal Physics, 3: 293. New York: Interscience Publishers, Inc., 1952.
9. Rosenbaum, H. S. and D. Turnbull. Metallographic Investigation of Precipitation of Silicon from Aluminum, 58-RL-2153. December, 1958.
10. Rosenbaum, H. S. and D. Turnbull. On the Precipitation of Silicon Out of a Supersaturated Aluminum-Silicon Solid Solution, 58-RL-1920. March, 1958.
11. Rosenbaum, H. S. "Precipitation of Silicon from a Supersaturated Aluminum-Silicon Solid Solution," Doctorate Thesis. Troy, New York: Rensselaer Polytechnic Institute. May, 1959.
12. Meussner, R. A. The Structure of Aluminum-Silicon Alloys, NRL-5341. July, 1959.
13. Meussner, R. A. "Isothermal Growth of Silicon Particles in an Aluminum Matrix." Doctorate Thesis. Carnegie Institute of Technology. 1953.
14. Glazov, V. M. and U. N. Vigdorovich. "On Diffusion-Free Crystallization of Metal Alloys," Doklady Akademii Nauk., S. S. S. R. 118: 924-927. February, 1958.

15. Hansen, M. Constitution of Binary Alloys, 2nd ed., 132-134. New York: McGraw-Hill, 1958.

16. Meussner, R. A. The Aluminum-Silicon Eutectic, NRL-5331. June, 1959.

17. Craighead, C. M., E. W. Cawthorne, and R. I. Jaffee. "Solution Rate of Solid Aluminum in Molten Al-Si Alloy," J. of Metals 7; AIME. Trans. 203: 81-87. 1955.

18. DePierre, V. and H. Berstein. "Grain Refinement of Aluminum-Silicon (5 per cent Si) and Aluminum-Silicon-Magnesium (7 per cent Si, 0.39 M_S) Casting Alloys," Trans. Am. Soc. Metals, 43: 635-643. 1951.

19. Smith, C. S. and L. Guttman. "Measurement of Internal Boundaries in Three-Dimensional Structures by Random Sectioning," J. of Metals, 5: 81-87. January, 1953.

20. Kehl, G. L. The Principles of Metallographic Laboratory Practice, 3rd ed. New York: McGraw-Hill, 1949.

21. Jetter, L. K. and R. F. Mehl. "Rate of Precipitation of Silicon from the Solid Solution of Silicon in Aluminum," AIME Trans., Institute of Metals Division, 152: 166-181. New York, 1943.

APPENDIX A

DISCUSSION OF APPLICATION OF CONVENTIONAL GRAIN SIZE MEASURING TECHNIQUES TO HEAT-TREATED Al-Si

Heyn's and Graff-Snyder's intercept methods of measuring grain size appeared promising until actually tried. The following questions arose concerning the acicular Si grains of low temperature annealed Al-Si:

1. When using a grid of lines superimposed on a magnified field, a single acicular crystal or grain is crossed by several grid lines. Should this be counted as one grain or should the number of times it is crossed by grid lines be considered the proper value?

2. Is it better to measure crystals per unit area, or crystals per unit length of line, or phase boundary crossings per unit length of line?

3. Is it necessary to measure the length to width ratio of the crystals?

These questions became meaningless when it was discovered that by each method of grain size measurement some samples which had received no heat treatment contained larger grains than some which obviously had undergone considerable heat treatment. Figure 5 illustrates this paradox.

The sample represented by photomicrograph A in Figure 5 was not heat treated, while those of photomicrographs B and C were heat treated at 275 C (527 F) for 0.56 days and 3.15 days, respectively. The sample shown in Figure 5 (photomicrograph C) had a duplex structure, the cause of which was not known. In this particular case it is quite easy to demonstrate the failure of grain size measurement to the analysis of annealing effect. Any test of annealing effect will obviously have to provide the same answer for both structures shown in Figure 5 (photomicrograph C).

Ambiguous results were obtained on grain size estimates made on samples of high annealing value, where the spheroidized shapes were more uniform. This can be seen in Table II. For these data, photomicrographs were enlarged to 2000 diameters on 8-1/2 x 11 prints. A transparent

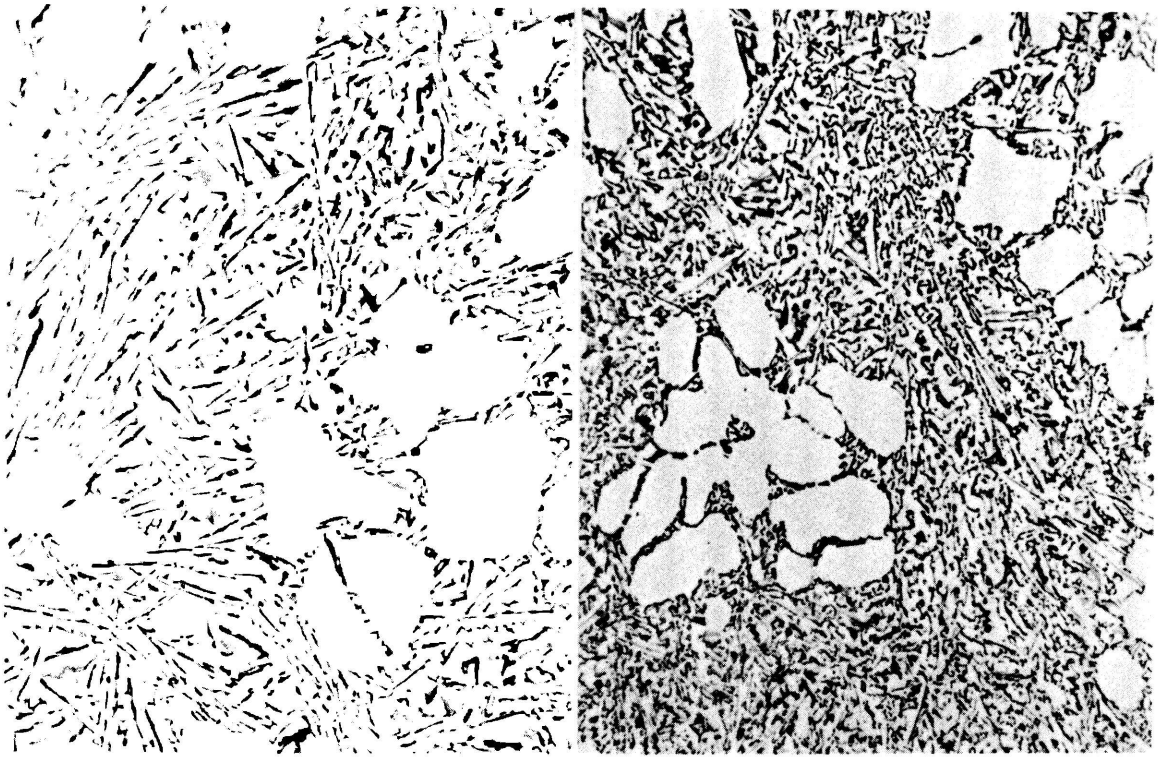

A B

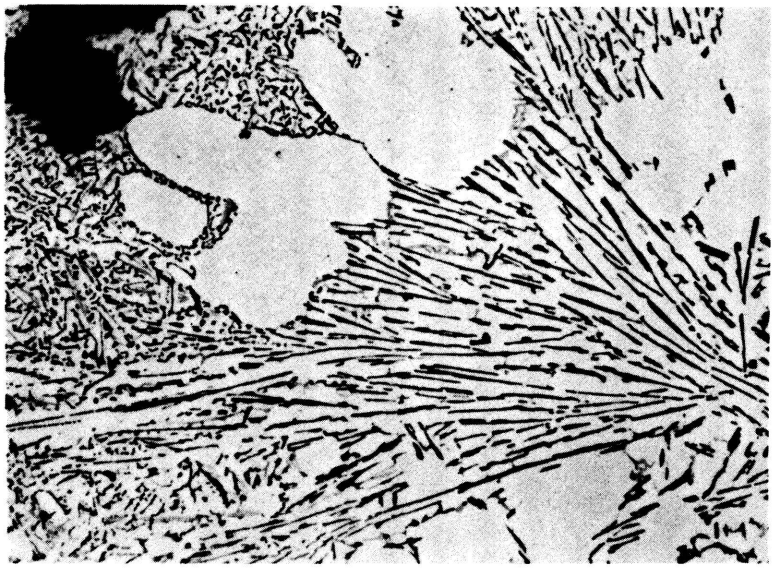

C

FIGURE 5

These Selected Photomicrographs Demonstrate the Complexity of the Problem of Measuring Annealing Effect. Photo A Has Received No Heat Treatment, Photo B Has Received 0.56 Days at 275 C, and Photo C Has Received 3.15 Days at 275 C.
Etched With 0.5% HF 750 X

AEC-GE RICHLAND, WASH.

grid with 5 mm line separations was laid over the prints. A count was then made of all of the Si crystals and all of the squares in the eutectic regions excluding the areas within the primary α grains. This provided data for crystals per square centimeter at 2000 diameters. All crystals intercepted by the grid lines were counted and this number was divided by the length of line in centimeters, again only within the eutectic regions.

TABLE II

GRAIN SIZE SUMMARY DETERMINED FROM PHOTOMICROGRAPHS AT 2000 DIAMETERS

Sample	Temperature °C	Temperature °F	Time Days	Crystals cm^{-2}	Crystal cm^{-1}	Annealing Number
A3G	404	759	10.0	1.22	0.504	24
A4G	404	759	17.8	1.21	0.632	25
A4H	404	759	56.2	1.58	0.660	27
A3I	404	759	100.0	0.86	0.409	28

When it became apparent no meaningful answers would come from use of these methods, an attempt was made to determine the size distribution and length to width ratio distribution of the grains in each sample. Photomicrographic prints at 2000 diameters were used for this study. A transparent overlay with lines scribed at 5 mm intervals was used as a guide. The length and width of each crystal of Si was measured. A record was made of the approximate total area and the ratio of the length and width of each crystal. This information when plotted on distribution curves would show the over-all pattern of grain sizes and shapes. Results from the first three photomicrographs treated in this way indicated good to fair agreement with actual annealing history. Time required for analyzing each photomicrograph was approximately 16 hours. The heat-treated samples numbered 195, and in addition there were 25 control samples, not heat treated. If it were possible to measure the standard samples and determine the balance by comparison with the standards, this would mean actual measurement of 32 photomicrographs of heat-treated samples and

4 controls. Because of the forecast time required and the time available this method of grain size determination was dropped.

DISCUSSION OF TEMPORARY CONTROL FAILURE ON HEAT-TREATING FURNACES

Midway in the long-term heat treatments of 56 and 100 days, the carbon cell battery in the Celect-Ray Controller became unreliable and required replacing. The instrument technician failed to standardize properly the unit against the voltage of the new carbon cell battery. Consequently, the Celect-Ray controller failed to maintain the temperature within the assigned limits. The override circuit within the Brown recorder provided some semblance of temperature control but this was higher in each case than was desired. For a period of five and one-half hours, until the error was discovered and corrected, the furnace temperatures cycled as follows:

	1	2	3	4	5	6
Assigned Temperature ^{o}C	250	275	303	333	367	404
Overrun Approximate Mean Temperature	263	288	320	362	417	450
Overrun Maximum Temperature	270	295	330	374	430	462
Overrun Minimum Temperature	250	273	301	342	400	441

Each cycle required 30 to 40 minutes.

At the time of this control malfunction, the 56-day samples had received 47 days' exposure, and the 100-day samples had received 79 days' exposure. The anneals were continued to full term at the assigned temperatures as the malfunction was considered to introduce little error. Extrapolation of known data indicated the effect of this short temperature excursion would be less than five per cent error in equivalent exposure time in the most severe condition which was that of the 56-day sample at 404 C (759 F). This would result in a change in annealing effect of a very small fraction of one unit on the annealing number scale. Later examinations of the samples' microstructure proved this prediction to be true. With

the exception of this one incident, the over-all temperature control was well within plus or minus 5 C at all temperatures.

EFFECT OF PROLONGED LEAD CONTACT ON THE MICROSTRUCTURE OF Al-Si

A small amount of lead can be held in solid solution in solid aluminum. This amount is not greater than 0.2 w/o lead at the monotectic temperature of 658.5 C (1217 F). No solubility of lead in aluminum is reported below this temperature. Lead and silicon are reported to be mutually and totally insoluble.[15] However, it is possible that prolonged contact between molten lead and the Al-Si samples could alter the microstructure. To investigate this possibility, two pieces of the virgin Al-Si material were annealed at 550 C (1022 F) for 3.16 days. This was a much more severe heat treatment than was given to any other sample. The first of these samples was heat-treated in air, the second was placed in contact with a pool of molten lead. Both were run in the same furnace on consecutive three-day periods. No lead was introduced into the furnace until the first sample had been removed. Upon completion of the anneal the samples were allowed to air cool. The microstructures of these samples are shown in Figures 6 and 7. Apparently there is some solubility of lead in aluminum at the temperature of 550 C (1022 F) since areas resembling specks of dirt between the Si crystals appeared after the heat treatment as shown in Figure 7. These areas of Figure 7 were attacked by a mild mixture of nitric and hydrofluoric acids (3 per cent and 2 per cent by volume in ethyl alcohol) applied with a cotton swab. Lead would be expected to be attacked by such a nitric acid mixture. The sample represented by Figure 6 had fewer specks between the Si crystals, and swabbing with the nitric-hydrofluoric acid mixture merely cleaned the surface of this sample. It is assumed, therefore, that these specks, shown in Figure 7 are small nodules of lead which were placed in solution in the aluminum by the heat treatment, and precipitated out again during air cooling of the sample.

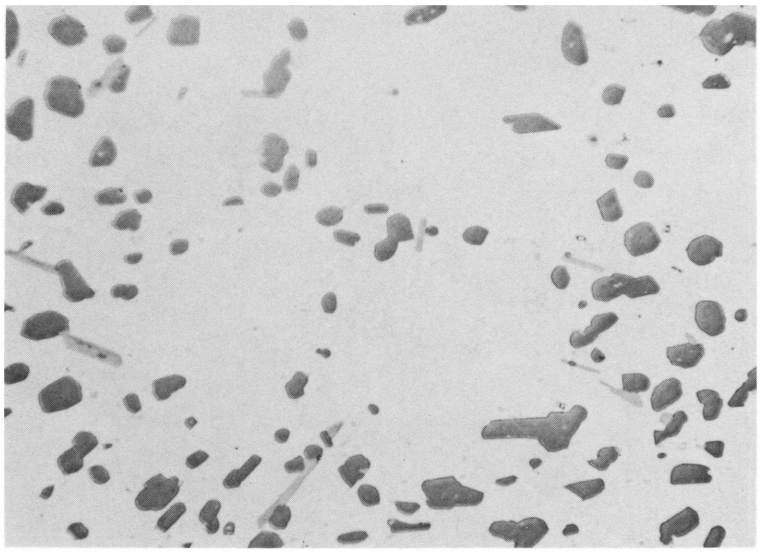

750 X

FIGURE 6

Microstructure of Al-Si Sample
After 3.16 Days At 550 C in Air
Etched with 0.5 Per Cent HF

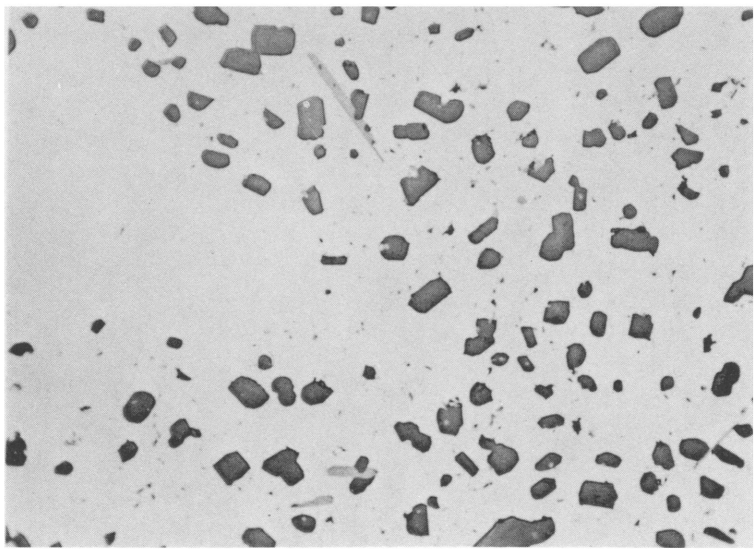

750 X

FIGURE 7

Microstructure of Al-Si Sample
After 3.16 Days at 550 C in Contact with Lead
Etched with 0.5 Per Cent HF

AEC-GE RICHLAND, WASH.

Detailed examination of these two samples revealed no other differences. It was concluded that heating samples in contact with molten lead for periods of time ranging from 15 minutes to 7-1/2 hours would not result in any significant change in spheroidization characteristics of the Si phase in Al-Si. It was assumed that Wood's metal when used at temperatures below the melting point of lead (327 C; 621 F) would have negligible effects on the microstructure of the Al-Si.

APPENDIX B

ANALYSIS OF REACTION KINETICS FOR SPHEROIDIZATION OF Si IN Al-Si

The kinetics of the Al-Si spheroidization reaction basically are those associated with grain growth since recrystallization is not involved. Reduction of surface energy provides the driving force for the Si particle growth. The reaction rates of both grain growth and diffusion are described by the reaction rate equation. Although the values for each term of this equation may differ between the separate processes of grain growth and of silicon diffusion through the aluminum, the same equation can be applied to the complex process where both diffusion and growth are involved. No attempt is made in this paper to separate the activation energies of the two steps involved in the process of spheroidization of the Si. Thus the activation energy obtained is for the entire process.

The general reaction rate or diffusion equation can be written

$$k = Ae^{-\frac{Q}{RT}} \tag{1}$$

where k is the reaction rate, A is a constant, and Q is the activation energy for the over-all process. R is the gas constant, and T is the absolute temperature in degrees Kelvin. When the logarithm of the reaction rate is plotted against the reciprocal of the absolute temperature, a straight line will result if the rate of reaction is controlled by a diffusion process. The slope of the line Q/R will then yield the value of the activation energy. The general rate equation can be rewritten as follows:

$$\ln k = \ln A + \frac{-Q}{RT} \tag{2}$$

$$\frac{Q}{RT} = \ln A - \ln k \tag{3}$$

$$\frac{1}{T} = \frac{R}{Q} \ln A - \frac{R}{Q} \ln k \tag{4}$$

If, in this process, we define N' as the absolute annealing value, then by substituting $\ln \frac{\Delta N'}{\Delta t}$ for ln k we obtain:

$$\frac{1}{T} = \frac{R}{Q} \ln A + \frac{R}{Q} \ln \frac{\Delta t}{\Delta N'} \tag{5}$$

$$\frac{1}{T} = \frac{R}{Q} \ln \frac{A}{\Delta N'} + \frac{R}{Q} \ln \Delta t \tag{6}$$

Substituting $A_{N'}$ for the term $\frac{R}{Q} \ln \frac{A}{\Delta N'}$:

$$\frac{1}{T} = A_{N'} + \frac{R}{Q} \ln \Delta t \tag{7}$$

In this form $A_{N'}$ will remain constant for a given value of $\Delta N'$ and will vary inversely with $\Delta N'$. For any given increase of N', or value of N' if the initial state was nonheat-treated, the reciprocal of absolute temperature is proportional to the natural logarithm of the time interval required for that change.

For convenience of plotting the following form of Equation (7) was used:

$$\frac{1000}{T} = A_N + b \log_{10} \Delta t \tag{8}$$

The term A_N is used instead of $A_{N'}$ to indicate the annealing values used are according to the arbitrary standards shown in Figure 3. It would be possible to relate the arbitrary annealing values to absolute annealing values. This has not been done here because the arbitrary scale had to be made to work first, and the further refinement of absolute values would have little practical value.

When completely assembled, the data presented in Table IV of this appendix was submitted to the statistician for analysis. The statistician's report provided the following values. The individual values for term "b" of Equation (8) according to data from the three groups of samples was: Series A: 0.1302; Series B: 0.1273; Series C: 0.1214. Combining data from Series A and B gave a value of 0.1215; and combining Series A, B,

and C gave a value for "b" of 0.1215. With this value for "b", the activation energy, Q, for the process is calculated to be -37,660 calories per gram mole, or -37,700 calories per gram mole when rounded off to three significant figures. As a comparison, the activation energy for the nucleation of Si in saturated aluminum, as given by Jetter and Mehl,[21] is -31,500 calories per gram mole.

Values for the intercept term, A_N, were computed statistically and are listed in Table III. The curve, fitted to these values by an orothogonal polynomial fit, is described by the equation:

$$A_N = 1.9675 - 0.01821N - 0.0026N^2$$

Calculated values for A_N from this equation are also shown in Table III. The standard error, obtained by a Root Mean Square Average, between values obtained from the equation and the raw values is 0.0179.

VALUES FOR A_N AS DETERMINED FOR INDIVIDUAL ANNEALING VALUES, N, AND CORRESPONDING VALUES OF A_N AS CALCULATED FROM THE FITTED EQUATION

N	A_N	A_N Cal.	Deviation	N	A_N	A_N Calc.	Deviation
1	1.9348	1.9490	+0.0142	15	1.6080	1.6358	+0.0278
2	1.9382	1.9300	-0.0082	16	1.5918	1.6095	+0.0177
3	1.9330	1.9105	-0.0225	17	1.5931	1.5827	-0.0104
4	1.9361	1.8905	-0.0456	18	1.5551	1.5554	+0.0003
5	1.8567	1.8700	+0.0133	19	1.5456	1.5276	-0.0180
6	1.8288	1.8489	+0.0201	20	1.5084	1.4993	-0.0091
7	1.8354	1.8273	-0.0081	21	1.4734	1.4704	-0.0030
8	1.7717	1.8052	+0.0335	22	1.4234	1.4410	+0.0180
9	1.7467	1.7826	+0.0359	23	1.4502	1.4111	-0.0391
10	1.7280	1.7594	+0.0314	24	1.3755	1.3807	+0.0052
11	1.7501	1.7357	-0.0144	25	1.3394	1.3498	+0.0104
12	1.7160	1.7115	-0.0045	26	1.3143	1.3183	+0.0040
13	1.7116	1.6868	-0.0248	27	1.2920	1.2864	-0.0056
14	1.6930	1.6616	-0.0314	28	1.2353	1.2538	+0.0185

When the individual values and the curve are plotted, as in Figure 11, a reasonable distribution pattern results. The fit along the entire length of the curve indicates the overlapped region of the annealing value scale was properly fitted. Further examination of Figure 11 shows a greater scatter of points for the lower values of N. This scatter of points, combined with the data presented in Figures 8, 9 and 10 of this appendix, indicates that Al-Si annealing values below 15 will be subject to increasing probable error. Estimations of annealing value below 15 would be considerably improved if a number of determinations were made and the results averaged. This prediction of error applies to only the arbitrary annealing values. The error in estimated temperature, as the discussion in the main text indicates, is approximately 30 C over the entire range of temperatures tested.

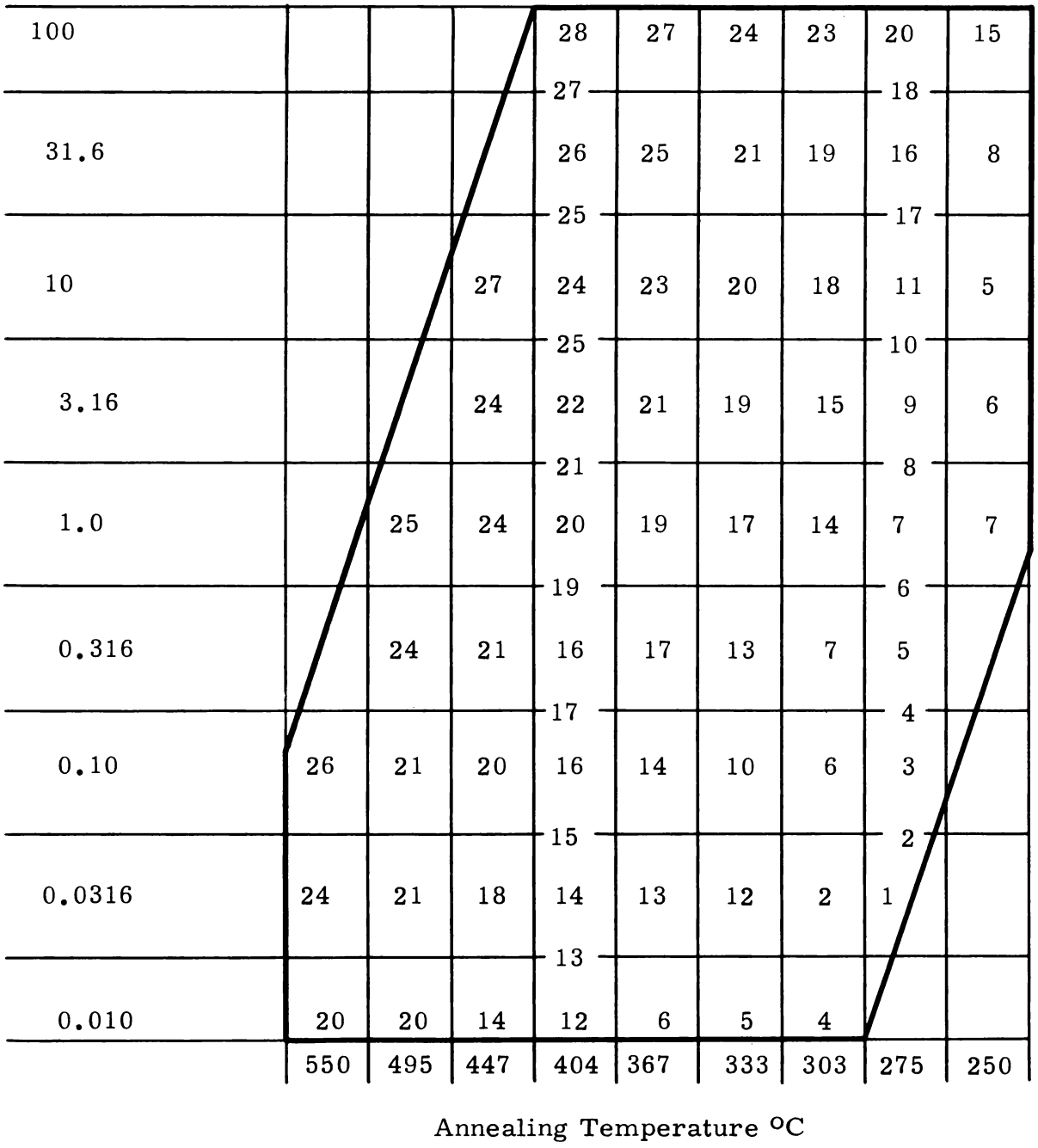

FIGURE 8

Simplified Arrhenius Plot. Annealing Values Were Acheived by the Various Heat Treatments Given Samples in Series A.

AEC-GE RICHLAND, WASH.

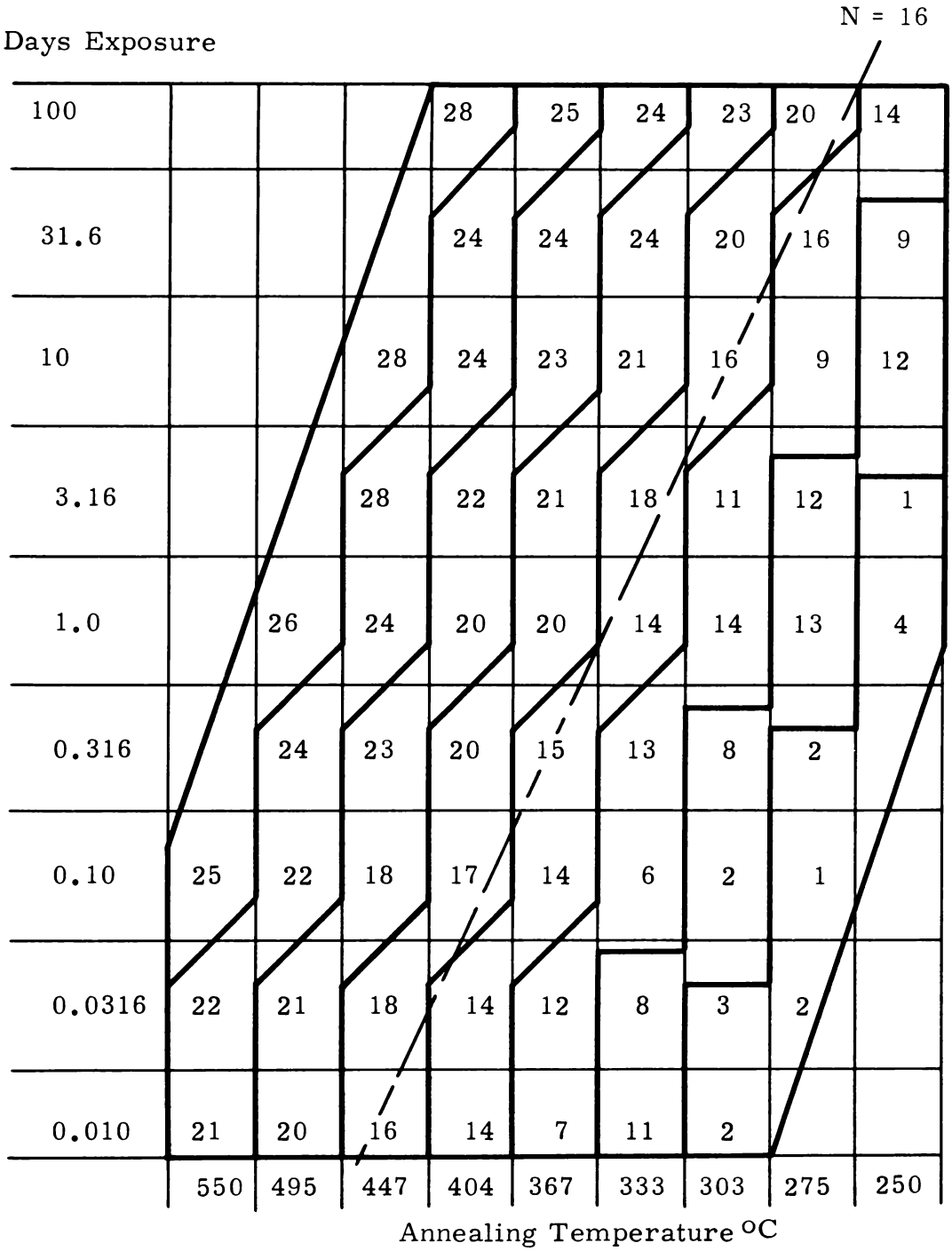

FIGURE 9

Simplified Arrhenius Plot. Annealing Values were Acheived by the Various Heat Treatments Given Samples in Series B

AEC-GE RICHLAND, WASH.

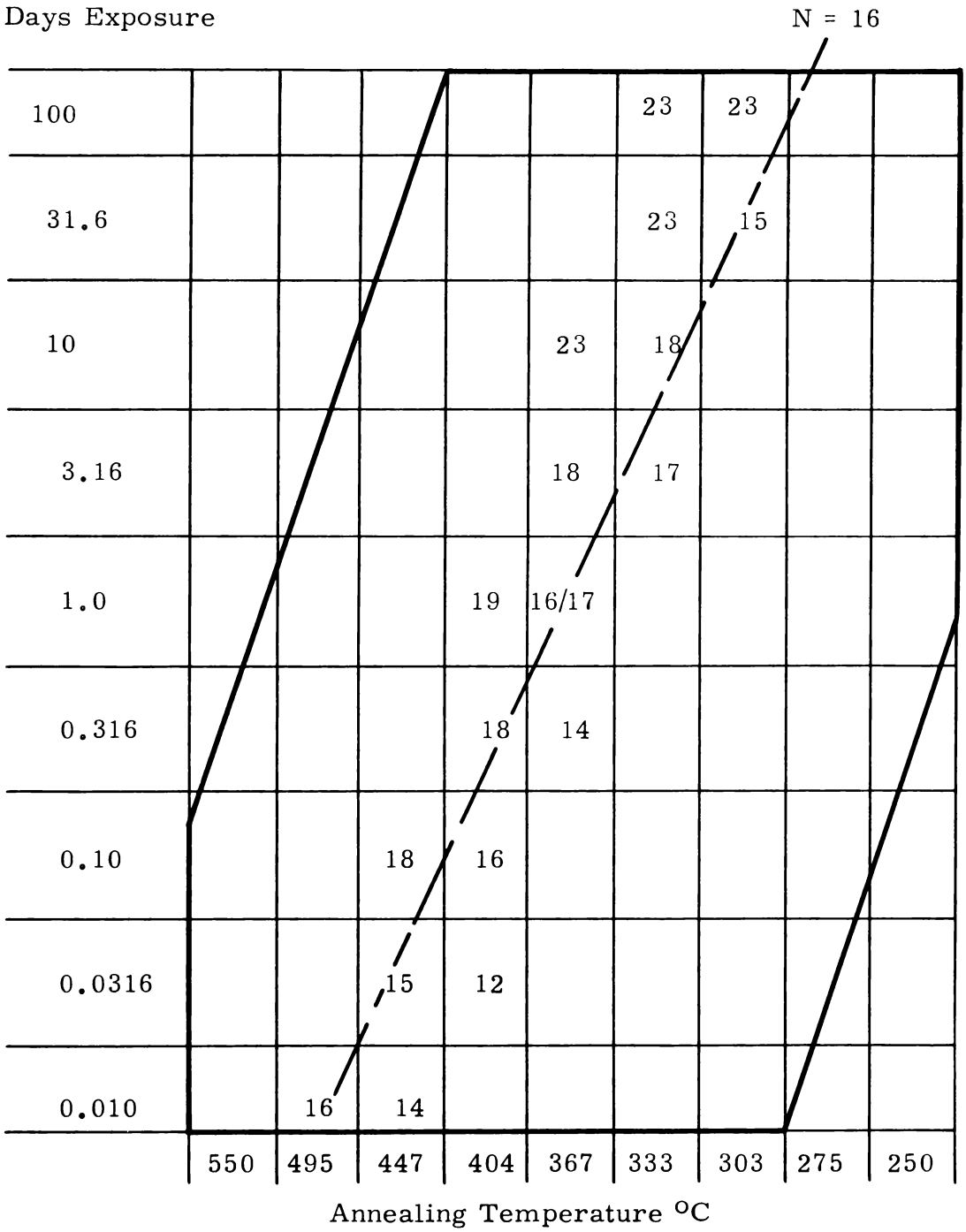

FIGURE 10

Simplified Arrhenius Plot. Annealing Values were Acheived by the Various Heat Treatments Given Samples in Series C.

AEC-GE RICHLAND, WASH.

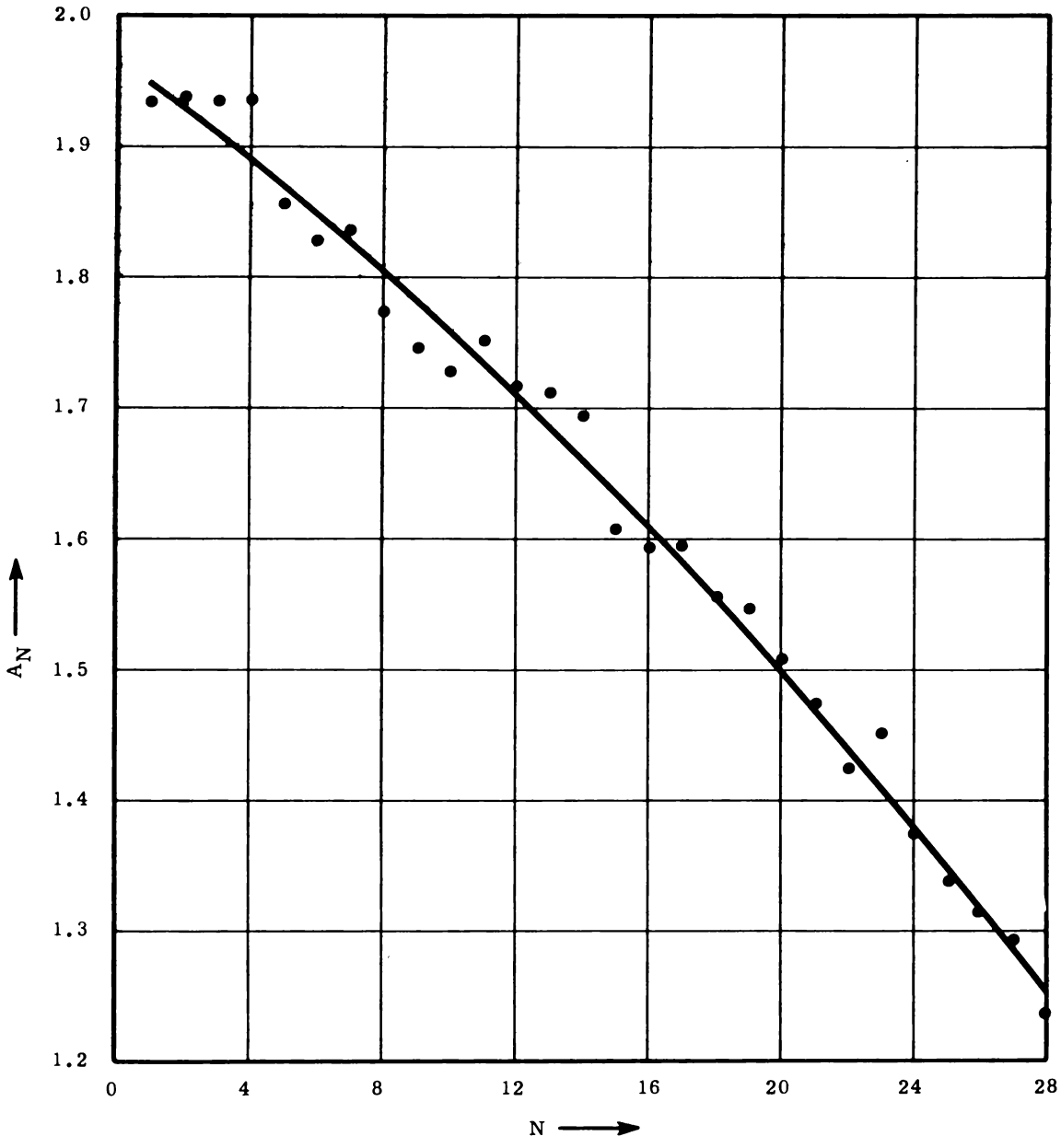

FIGURE 11

Values for the Intercept Term A_N
Versus Annealing Values N, and a Corresponding Plot
of the Fitted Equation $A_N = 1.9675 - 0.01821N - 0.0026\ N^2$.

AEC-GE RICHLAND, WASH

TABLE IV

SUMMARY OF ANNEALING CONDITIONS AND RESULTANT ANNEALING VALUES

Sample No.	Annealing Conditions		Relative Annealing Value	Sample No.	Annealing Conditions		Relative Annealing Value
	Time Days	Temp. °C			Time Days	Temp. °C	
A1A	0.0315	275	1	A4A	0.0178	404	13
A1B	0.100	275	3	A4B	0.056	404	15
A1C	0.315	275	5	A4C	0.176	404	17
A1D	1.00	275	7	A4D	0.560	404	19
A1E	3.15	275	9	A4E	1.75	404	21
A1F	10.0	275	11	A4F	5.60	404	25
A1G	31.6	275	16	A4G	17.8	404	25
A1H	100.0	275	20	A4H	56.2	404	27
A2A	0.056	275	2	A5A	1.00	250	7
A2B	0.175	275	4	A5B	3.16	250	6
A2C	0.560	275	6	A5C	10.0	250	5
A2D	1.75	275	8	A5D	31.6	250	8
A2E	5.60	275	10	A5E	100.0	250	15
A2F	17.54	275	17				
A2G	56.2	275	18	A6A	0.010	303	4
				A6B	0.0315	303	2
A3A	0.010	404	12	A6C	0.100	303	6
A3B	0.0316	404	14	A6D	0.316	303	7
A3C	0.100	404	16	A6E	1.00	303	14
A3D	0.316	404	16	A6F	3.16	303	15
A3E	1.00	404	20	A6G	10.0	303	18
A3F	3.15	404	22	A6H	31.6	303	19
A3G	10.0	404	24	A6I	100.0	303	23
A3H	31.6	404	26				
A3I	100.0	404	28				

TABLE IV (contd.)

Sample No.	Annealing Conditions: Time Days	Annealing Conditions: Temp. °C	Relative Annealing Value	Sample No.	Annealing Conditions: Time Days	Annealing Conditions: Temp. °C	Relative Annealing Value
A7A	0.010	333	5	A10A	0.010	550	20
A7B	0.0315	333	12	A10B	0.0315	550	24
A7C	0.100	333	10	A10C	0.100	550	26
A7D	0.318	333	13	A10D	0.010	478	16
A7E	1.00	333	17	A10E	0.0315	478	17
A7F	3.16	333	19	A10F	0.100	478	22
A7G	10.0	333	20	A10G	0.315	478	22
A7H	31.6	333	21	A10H	1.00	478	26
A7I	100.0	333	24				
				A11A	0.010	550	21
A8A	0.010	367	6	A11B	0.0318	550	24
A8B	0.0316	367	13	A11C	0.100	550	25
A8C	0.100	367	14				
A8D	0.316	367	17	A12A	0.010	495	20
A8E	1.00	367	19	A12B	0.0315	495	21
A8F	3.16	367	21	A12C	0.100	495	21
A8G	10.00	367	23	A12D	0.315	495	24
A8H	31.6	367	25	A12E	1.00	495	25
A8I	100.0	367	27				
				A13A	0.010	447	14
A9A	0.010	423	13	A13B	0.0315	447	18
A9B	0.0315	423	12	A13C	0.100	447	20
A9C	0.100	423	16	A13D	0.316	447	21
A9D	0.32	423	20	A13E	1.01	447	24
A9E	1.00	423	20	A13F	3.16	447	24
A9F	3.15	423	23	A13G	10.00	447	28
A9G	10.0	423	24				

TABLE IV (contd.)

Sample No.	Annealing Conditions: Time Days	Annealing Conditions: Temp. °C	Relative Annealing Value	Sample No.	Annealing Conditions: Time Days	Annealing Conditions: Temp. °C	Relative Annealing Value
B1A	0.010	303	2	B4A	0.010	404	14
B1B	0.0315	303	3	B4B	0.0316	404	14
B1C	0.100	275	1	B4C	0.100	367	14
B1D	0.316	275	2	B4D	0.316	367	15
B1E	1.00	250	4	B4E	1.00	333	14
B1F	3.15	250	1	B4F	3.16	333	18
B1G	0.0315	275	2	B4G	10.00	303	16
				B4H	31.6	303	20
B2A	0.010	333	11	B4I	100.0	275	20
B2B	0.0315	333	8				
B2C	0.100	303	2	B5A	0.010	423	11
B2D	0.316	303	8	B5B	0.0315	423	13
B2E	1.00	275	13				
B2F	3.15	275	12	B6A	0.010	478	15
B2G	10.0	250	12	B6B	0.0315	478	19
B2H	31.6	250	9	B6C	0.100	423	17
				B6D	0.315	423	20
B3A	0.010	367	7				
B3B	0.032	367	12	B7A	0.010	550	20
B3C	0.100	333	6	B7B	0.0315	550	23
B3D	0.318	333	13	B7C	0.100	478	22
B3E	1.00	303	14	B7D	0.315	478	20
B3F	3.16	303	11	B7E	1.00	423	22
B3G	10.00	275	9	B7F	3.15	423	24
B3H	31.6	275	16				
B3I	100.0	250	14	B8A	0.100	550	25

TABLE IV (contd.)

Sample No.	Annealing Conditions Time Days	Temp. °C	Relative Annealing Value	Sample No.	Annealing Conditions Time Days	Temp. °C	Relative Annealing Value
B8B	1.00	478	25	B11F	3.16	447	26
B8C	10.00	423	26	B11G	10.0	404	24
				B11H	31.6	404	26
B9A	0.010	447	16	B11I	100.0	367	25
B9B	0.0315	447	18				
B9C	0.100	404	17	B12A	0.100	550	25
B9D	0.316	404	20	B12B	1.00	495	26
B9E	1.00	367	20	B12C	10.00	447	28
B9F	3.16	367	21	B12D	100.0	404	28
B9G	10.00	333	21				
B9H	31.6	333	24	C1	0.010	478	11
B9I	100.0	303	23	C2	0.010	423	10
				C3	0.0316	423	12
B10A	0.010	495	20	C4	0.0316	404	12
B10B	0.0315	495	21	C5	0.100	423	13
B10C	0.100	447	18	C6	0.100	404	16
B10D	0.316	447	23	C7	0.316	404	18
B10E	1.00	404	20	C8	0.316	367	14
B10F	3.15	404	22	C9	1.00	404	19
B10G	10.00	367	23	C10	1.00	367	16
B10H	31.6	367	24	C11	3.16	367	18
B10I	100.0	333	24	C12	3.16	333	17
				C13	10.00	367	23
B11A	0.010	550	21	C14	10.00	333	18
B11B	0.0318	550	22	C15	31.6	333	23
B11C	0.100	495	22	C16	31.6	303	15
B11D	0.315	495	24	C17	100.0	333	23
B11E	1.01	447	24	C18	100.0	303	23

TABLE IV (contd.)

Sample No.	Annealing Conditions		Relative Annealing Value
	Time Days	Temp. °C	
C19	0.010	495	16
C20	0.010	447	14
C21	0.0315	447	15
C22	0.100	447	18

INTERNAL DISTRIBUTION

Copy Number

1 F. W. Albaugh
2 W. K. Alexander
3 G. S. Allison
4 T. W. Ambrose
5 P. A. Ard
6 J. A. Ayres
7 A. L. Bement
8 T. K. Bierlein - B. Mastel
9 C. L. Boyd
10 R. V. Bowersock
11 J. H. Brown
12 S. H. Bush
13 J. J. Cadwell
14 R. L. Call
15 L. J. Chockie
16 D. R. Dickinson
17 R. L. Dillon
18 E. A. Evans
19 M. C. Fraser
20 R. M. Fryar
21 S. M. Gill
22 J. W. Goffard
23 O. H. Greager
24 B. Griggs
25 W. J. Gruber
26 A. E. Guay
27 L. A. Hartcorn
28 H. Harty
29 K. D. Hayden
30 J. J. Holmes
31 R. S. Kemper
32 B. S. Kosut
33 W. K. Kratzer
34 J. J. Laidler
35 G. A. Last
36 R. D. Leggett
37 R. J. Lobsinger
38 L. H. McEwen
39 M. E. McMahan
40 J. E. Minor
41 R. G. Nelson - E. A. Smith
42 D. P. O'Keefe
43 R. E. Olson
44 H. J. Pessl
45 F. B. Quinlan

INTERNAL DISTRIBUTION (contd.)

Copy Number	
46	J. W. Riches
47	G. W. Riederman
48	G. L. Rogers
49 - 51	R. K. Sharp
52	W. I. Steinkamp
53	R. W. Stewart
54	R. Teats
55	R. A. Thiede
56	I. D. Thomas
57	J. C. Tobin
58	R. H. Todd
59	J. W. Weber
60	K. R. Wheeler
61	R. G. Wheeler
62	O. J. Wick
63	N. G. Wittenbrock
64	F. W. Woodfield
65	G. E. Zima
66	H. F. Zuhr
67	300 Files
68	Record Center
69 - 99	Extra

EXTERNAL DISTRIBUTION (Special)

Copy Number	
1	HOO Technical Technical Information Library

EXTERNAL DISTRIBUTION

Number of Copies	
3	Aberdeen Proving Ground
1	Aerojet-General Corporation
1	Aerojet-General Nucleonics
1	Aeroprojects Incorporated
2	ANP Project Office, Convair, Fort Worth
1	Alco Products, Inc.
1	Allis-Chalmers Manufacturing Company
1	Allis-Chalmers Manufacturing Company, Washington
1	Allison Division-GMC
10	Argonne National Laboratory
1	Armour Research Foundation
1	Army Ballistic Missile Agency
1	AEC Scientific Representative, Belgium
1	AEC Scientific Representative, France
1	AEC Scientific Representative, Japan
3	Atomic Energy Commission, Washington

EXTERNAL DISTRIBUTION (contd.)

Number of Copies	
4	Atomic Energy of Canada Limited
4	Atomics International
4	Babcock and Wilcox Company
2	Battelle Memorial Institute
1	Beryllium Corporation
1	Bridgeport Brass Company
1	Bridgeport Brass Company, Adrian
2	Brookhaven National Laboratory
1	Brush Beryllium Company
1	Bureau of Mines, Albany
1	Bureau of Ships (Code 1500)
1	Carborundum Company
3	Chicago Operations Office
1	Chicago Patent Group
1	Clevite Corporation
1	Combustion Engineering, Inc.
1	Combustion Engineering, Inc. (NRD)
1	Convair-General Dynamics Corporation, San Diego
1	Defence Research Member
1	Denver Research Institute
2	Department of the Army, G-2
1	Dow Chemical Company (Rocky Flats)
4	duPont Company, Aiken
1	duPont Company, Wilmington
1	Frankford Arsenal
1	Franklin Institute of Pennsylvania
2	General Atomic Division
2	General Electric Company (ANPD)
1	General Electric Company, St. Petersburg
1	General Nuclear Engineering Corporation
1	Glasstone, Samuel
1	Goodyear Atomic Corporation
2	Iowa State University
2	Jet Propulsion Laboratory
1	Johns Hopkins University (ORO)
3	Knolls Atomic Power Laboratory
3	Los Alamos Scientific Laboratory
1	Los Alamos Scientific Laboratory (Sesonske)
1	M & C Nuclear, Inc.
1	Mallinckrodt Chemical Works
1	Maritime Administration
1	Martin Company
1	Mound Laboratory
1	NASA Lewis Research Center
2	National Bureau of Standards
1	National Bureau of Standards (Library)

EXTERNAL DISTRIBUTION (contd.)

Number of Copies	
1	National Carbon Company
2	National Lead Company of Ohio
3	Naval Research Laboratory
1	New Brunswick Area Office
1	New York Operations Office
1	Northern Research and Engineering Corporation
1	Nuclear Development Corporation of America
1	Nuclear Materials and Equipment Corporation
1	Nuclear Metals, Inc.
1	Oak Ridge Institute of Nuclear Studies
2	Office of Naval Research
1	Office of Naval Research (Code 422)
1	Olin Mathieson Chemical Corporation
1	Ordnance Materials Research Office
1	Ordnance Tank-Automotive Command
1	Patent Branch, Washington
4	Phillips Petroleum Company (NRTS)
1	Picatinny Arsenal
1	Power Reactor Development Company
3	Pratt and Whitney Aircraft Division
1	Rensselaer Polytechnic Institute
2	Sandia Corporation, Albuquerque
1	Sandia Corporation, Livermore
1	Stevens Institute of Technology (Comstock)
1	Sylvania Electric Products, Inc.
1	Technical Research Group
1	Tennessee Valley Authority
2	Union Carbide Nuclear Company (ORGDP)
5	Union Carbide Nuclear Company (ORNL)
1	Union Carbide Nuclear Company (Paducah Plant)
1	USAF Project RAND
1	U. S. Geological Survey, Denver
1	U. S. Geological Survey, Menlo Park
1	U. S. Geological Survey, Washington
1	U. S. Naval Postgraduate School
1	U. S. Patent Office
2	University of California, Berkeley
2	University of California, Livermore
1	University of Puerto Rico
1	Watertown Arsenal
4	Westinghouse Bettis Atomic Power Laboratory
1	Westinghouse Electric Corporation
8	Wright Air Development Division
1	Yankee Atomic Electric Company
325	Division of Technical Information Extension